MULTIBODY DYNAMICS 2007, ECCOMAS Thematic Conference
C.L. Bottasso, P. Masarati, L. Trainelli (eds.)
Milano, Italy, 25–28 June 2007

ON DERIVING HIGHER-ORDER AND ENERGY-MOMENTUM-CONSISTENT TIME-STEPPING-SCHEMES FOR THERMO-VISCOELASTODYNAMICS FROM A NEW HYBRID SPACE-TIME GALERKIN METHOD

Michael Groß* **and Peter Betsch**†

Chair of Computational Mechanics, Department of Mechanical Engineering,
University of Siegen, Paul-Bonatz-Str. 9-11, D-57068 Siegen, Germany
webpage: `http://www.mb.uni-siegen.de/fb11/nm`
e-mail: *`gross@imr.mb.uni-siegen.de`, †`betsch@imr.mb.uni-siegen.de`

Keywords: Multi-Physics Problems, Space-Time Finite Element Methods, Time-Stepping Algorithms, Energy-Momentum Consistency, Higher-Order Accuracy.

Abstract. *A spatial discretisation of flexible solid bodies using the finite element method is a standard procedure in mechanical engineering. Finite element methods in time also have many advantages. For example, higher-order accurate time approximations can be obtained in a natural way, and it is well-known that continuous Galerkin (cG) methods in time are energy-consistent for equations of motion of dynamical systems. Hence, the cG method is very convenient to construct higher-order and energy-momentum-conserving time integrators for nonlinear elastodynamics. These time integrators, derived from the enhanced Galerkin (eG) method, turned out to be well suited for computing long time runs. The reason is the unconditionally numerical stability of energy-momentum-conserving integrators for conservative problems. In general, standard methods show a stability bound in dependence on the time step size. According to F. Armero and L. Noels, energy-momentum-consistent time integrators are of great advantage for simulating motions of plastic materials. The energy dissipation is guaranteed independent of the time step size, in contrast to conditionally stable standard methods. In this paper, we show that an energy-consistent simulation is also advantageous for dynamics with dissipation arising from conduction of heat and from a viscous material law. We consider Fourier's law of heat conduction, and a nonlinear finite thermo-viscoelastic material model, according to S. Reese and S. Govindjee. We derive the space-time weak evolution equations for the deformation, the momentum, the entropy and the viscous internal variable directly from an a priori stability estimate with respect to a Lyapunov function. This Lyapunov function coincides with the total energy relative to the equilibrium state of this dynamical system. In the discrete setting, the energy-consistency is accomplished by using a new enhanced hybrid Galerkin (ehG) method, in conjunction with proper time approximations of the constitutive laws. We obtain time-stepping algorithms, which fulfil the a priori stability estimate exactly, and independent of the time step size. This guarantees unconditionally numerical stability.*

1 INTRODUCTION

In this section, we introduce the used notation, and the geometrical concepts pertaining to the Lagrangian description of motions under the influence of thermo-mechanical coupling.

1.1 Preliminaries

Let $\mathbb{R}$ denote the set of real numbers, and $1 \leqslant n_{\text{dim}} \leqslant 3$ the space dimension. We denote by $\mathscr{A}$ the real vector space of columns $\boldsymbol{a} = [a^1, \dots, a^{n_{\text{dim}}}]$. We consider each column $\boldsymbol{a} \in \mathscr{A}$ as a point in the continuum with respect to a reference frame, located in the origin $\boldsymbol{o} = [0, \dots, 0]$. We refer to the space $\mathscr{A}$ as ambient space. Covectors in the dual space $\mathscr{A}^*$ are considered as row vectors $\boldsymbol{a}^* = [a_1 \dots a_{n_{\text{dim}}}]$, whose entries are defined via the Kronecker symbols as $a_j = a^i \delta_{ij}$. Summation over repeated indices is understood.

1.2 Kinematical aspects of deformation and motion

Denoting by the set $\mathscr{T} = [t_0, T] \subset \mathbb{R}_+$ the time interval of interest, we consider the reference configuration of the body at initial time $t_0 \in \mathscr{T}$ as an bounded open set $\mathcal{B}_0 \subset \mathscr{A}$. Hence, points in $\mathscr{B}_0$ are identified as column vectors $\boldsymbol{X} \in \mathscr{B}_0$. We assume a Dirichlet boundary $\partial_\varphi \mathscr{B}_0 \subset \partial \mathscr{B}_0$ on the piecewise smooth boundary $\partial \mathscr{B}_0$ of the reference configuration, on which points are hold fixed. The current configuration of the body at fixed time $t \in \mathscr{T}$ is a bounded open set $\mathscr{B}_t \subset \mathscr{A}$. An element $\boldsymbol{x} \in \mathscr{B}_t$ coincides with the deformation $\boldsymbol{\varphi}_t(\boldsymbol{X})$ of the corresponding point $\boldsymbol{X} \in \mathscr{B}_0$. The right Cauchy-Green tensor

$$[\boldsymbol{C}_t(\boldsymbol{X})]_{AB} = [\boldsymbol{F}_t^T(\boldsymbol{X})]_A{}^a \delta_{ab} \, [\boldsymbol{F}_t(\boldsymbol{X})]^b{}_B \tag{1}$$

determines the stretch in $\mathscr{B}_t$ with respect to tangent vectors $\boldsymbol{W}$ at $\mathscr{B}_0$. The tensor $\boldsymbol{F}_t(\boldsymbol{X})$ denotes the gradient $\nabla \boldsymbol{\varphi}_t(\boldsymbol{X})$ of the deformation, called the deformation gradient. Its determinant $J_t(\boldsymbol{X})$ is greater than zero, at all points of $\boldsymbol{X} \in \mathscr{B}_0$. A motion of the body is a curve $\boldsymbol{\varphi}(t) = \boldsymbol{\varphi}_t$ of deformations. At fixed time $t \in \mathscr{T}$, the deformation velocity $\boldsymbol{v}_t = \dot{\boldsymbol{\varphi}}_t$ denotes a tangent vector of the motion. The kinetic energy

$$\mathcal{T}(t) = \frac{1}{2} \int_{\mathscr{B}_0} \rho_0(\boldsymbol{X}) \, [\boldsymbol{v}_t(\boldsymbol{X})]^a \, \delta_{ab} \, [\boldsymbol{v}_t(\boldsymbol{X})]^b = \frac{1}{2} \int_{\mathscr{B}_0} [\boldsymbol{\pi}_t(\boldsymbol{X})]_b \, [\boldsymbol{v}_t(\boldsymbol{X})]^b \tag{2}$$

of the body defines the conjugated momentum $\boldsymbol{\pi}_t = \rho_0 \boldsymbol{v}_t^*$ of the body as vector in the cotangent space of the motion. The field ρ_0 denotes the body density in $\mathscr{B}_0$.

1.3 The temperature field of the body

The absolute temperatures $\Theta_t(\boldsymbol{X})$ at points $\boldsymbol{X} \in \mathscr{B}_0$ defines the body temperature field. We assume a piecewise smooth Dirichlet boundary $\partial_\Theta \mathscr{B}_0 \subset \partial \mathscr{B}_0$ on which absolute temperatures coincide with the constant environment temperature Θ_∞. The gradient $\nabla \Theta_t(\boldsymbol{X})$ of the temperature field defines a cotangent vector at the point $\boldsymbol{X} \in \mathscr{B}_0$. We refer to the curve $\Theta(t) = \Theta_t$ as the temperature evolution. The relative temperature field ϑ_t, which designates the temperature differences $\Theta_t(\boldsymbol{X}) - \Theta_\infty$ at all points $\boldsymbol{X} \in \mathscr{B}_0$, lies in the tangent space at the temperature evolution, as also the temperature velocity field $\dot{\Theta}_t$.

1.4 The concept of stress and entropy

In this work, we consider isotropic thermo-elastic material with fading memory properties. This memory is modelled by a symmetric tensor-valued internal variable $\boldsymbol{\Gamma}_t(\boldsymbol{X})$ (cp. Ref. [4]).

Accordingly, the family $\boldsymbol{\Lambda}_t = (\Theta_t, \boldsymbol{C}_t, \boldsymbol{\Gamma}_t)$ of fields determines the free energy $\Psi(\boldsymbol{\Lambda}_t(\boldsymbol{X}))$ of the body at each point $\boldsymbol{X} \in \mathscr{B}_0$. Since the memory effect may not affect the elastic properties, the free energy depend directly only on the product tensor $\boldsymbol{C}_t(\boldsymbol{X})\,\boldsymbol{\Gamma}_t^{-1}(\boldsymbol{X})$. Considering the free energy at the time curve $\boldsymbol{\Lambda}_X(t) = \boldsymbol{\Lambda}_t(\boldsymbol{X})$ of any point $\boldsymbol{X} \in \mathscr{B}_0$, the time rate of change

$$\dot{\Psi}_t(\boldsymbol{X}) = \frac{\partial \Psi(\boldsymbol{\Lambda}_t(\boldsymbol{X}))}{\partial \Theta}\,\dot{\Theta}_t(\boldsymbol{X}) + \frac{\partial \Psi(\boldsymbol{\Lambda}_t(\boldsymbol{X}))}{\partial C_{AB}}\,[\dot{\boldsymbol{C}}_t(\boldsymbol{X})]_{AB} + \frac{\partial \Psi(\boldsymbol{\Lambda}_t(\boldsymbol{X}))}{\partial \Gamma_{AB}}\,[\dot{\boldsymbol{\Gamma}}_t(\boldsymbol{X})]_{AB} \quad (3)$$

of the free energy defines their partial derivatives as cotangent vectors $-\eta_t(\boldsymbol{X}), \boldsymbol{S}_t(\boldsymbol{X})/2$ and $-\boldsymbol{\Upsilon}_t(\boldsymbol{X})$ at this time curve, respectively. By definition, these cotangent vectors are associated with the tangent vectors $\dot{\Theta}_t(\boldsymbol{X}), \dot{\boldsymbol{C}}_t(\boldsymbol{X})$ and $\dot{\boldsymbol{\Gamma}}_t(\boldsymbol{X})$, respectively. The cotangent vector $\eta_t(\boldsymbol{X})$ denotes the entropy, and $\boldsymbol{S}_t(\boldsymbol{X})$ represents the second Piola-Kirchhoff stress tensor. To the tensor $\boldsymbol{\Upsilon}_t(\boldsymbol{X})$, we refer to as non-equilibrium stress tensor. The second term of Eq. (3) is designated as the density $p_t^{\text{int}}(\boldsymbol{X})$ of the power $\mathcal{P}^{\text{int}}(t)$ at time $t \in \mathscr{T}$, done by the stress field on $\mathscr{B}_0$. By using the chain rule of differentiation, we obtain

$$p_t^{\text{int}}(\boldsymbol{X}) = \delta_{ac}[\boldsymbol{F}_t(\boldsymbol{X})]^c{}_B\,[\boldsymbol{S}_t(\boldsymbol{X})]^{BA}\,[\dot{\boldsymbol{F}}_t(\boldsymbol{X})]^a{}_A = [\boldsymbol{P}_t^*(\boldsymbol{X})]_a{}^A\,[\dot{\boldsymbol{F}}_t(\boldsymbol{X})]^a{}_A \quad (4)$$

We refer to the tensor $\boldsymbol{P}_t^*(\boldsymbol{X})$ as covariant first Piola-Kirchhoff stress tensor. It is the cotangent vector corresponding to the tangent vector $\dot{\boldsymbol{F}}_t(\boldsymbol{X})$.

1.5 The balance principles

According to the balance of mechanical energy, the sum of the rate of kinetic energy $\mathcal{T}(t)$ and the stress power $\mathcal{P}^{\text{int}}(t)$ coincide with the external mechanical power $\mathcal{P}^{\text{ext}}(t)$, done by the acting forces. In the Lagrangian description, this balance equation is equivalent to

$$\int_{\mathscr{B}_0} \rho_0(\boldsymbol{X})[\boldsymbol{v}_t^*(\boldsymbol{X})]_a\,[\dot{\boldsymbol{v}}_t(\boldsymbol{X})]^a + \int_{\mathscr{B}_0} [\boldsymbol{P}_t^*(\boldsymbol{X})]_a{}^A[\dot{\boldsymbol{F}}_t(\boldsymbol{X})]^a{}_A = \int_{\partial\mathscr{B}_0} [\boldsymbol{v}_t^*(\boldsymbol{X})]_a\,[\boldsymbol{t}_t(\boldsymbol{X})]^a \quad (5)$$

where $\boldsymbol{t}_t$ denotes the first Piola-Kirchhoff traction vector field for points on the traction boundary $\boldsymbol{X} \in \partial\mathscr{B}_0 \setminus \partial_\varphi\mathscr{B}_0$. First, we apply the Piola-Kirchhoff theorem and Gauss' divergence theorem for transforming the external mechanical power. Then, we take into account the definition of the deformation velocity, and arrive at the partial differential equation system

$$\boxed{\begin{array}{rcl} \dot{\boldsymbol{\varphi}}_t(\boldsymbol{X}) & = & \boldsymbol{v}_t(\boldsymbol{X}) \\ \dot{\boldsymbol{\pi}}_t(\boldsymbol{X}) & = & \mathrm{DIV}[\boldsymbol{P}_t^*(\boldsymbol{X})] \end{array}} \quad (6)$$

for all points $\boldsymbol{X} \in \mathscr{B}_0$. The operator DIV denotes the divergence. This system of equations represents the local form of the equations of motion in the Lagrangian setting. The temperature evolution follows from the righthand side of the Lagrangian form of the second law of thermodynamics at each point $\boldsymbol{X} \in \mathscr{B}_0$, given by

$$\int_{\mathscr{B}_0} \frac{D_t^{\text{tot}}(\boldsymbol{X})}{\Theta_t(\boldsymbol{X})} = \int_{\mathscr{B}_0} \dot{\eta}_t(\boldsymbol{X}) + \int_{\partial\mathscr{B}_0} [\boldsymbol{N}_0(\boldsymbol{X})]_A\,[\boldsymbol{H}_t(\boldsymbol{X})]^A \geqslant 0 \quad (7)$$

The field $D_t^{\text{tot}} : \mathscr{B}_0 \to \mathbb{R}$ denotes the total production of entropy, called total dissipation. The vector $\boldsymbol{N}_0(\boldsymbol{X})$ designates the outward normal at a point $\boldsymbol{X} \in \partial\mathscr{B}_0$. We denote by $\boldsymbol{H}_t(\boldsymbol{X})$ the assumed Piola-Kirchhoff entropy flux $\boldsymbol{Q}_t(\boldsymbol{X})/\Theta_t(\boldsymbol{X})$ at the point $\boldsymbol{X} \in \mathscr{B}_0$, where $\boldsymbol{Q}_t(\boldsymbol{X})$

denotes the Piola-Kirchhoff heat flux. The total dissipation $D_t^{\text{tot}}(\boldsymbol{X})$ is split into an internal dissipation $D_t^{\text{int}}(\boldsymbol{X})$ associated with a dissipative material law, and the dissipation

$$D_t^{\text{con}}(\boldsymbol{X}) = -[\nabla \Theta_t(\boldsymbol{X})]_A \, [\boldsymbol{H}_t(\boldsymbol{X})]^A \tag{8}$$

arising from conduction of heat. After applying Gauss' divergence theorem to the boundary integral in Eq. (7), we take into account the dissipation $D_t^{\text{con}}(\boldsymbol{X})$, according to Eq. (8). In this way, we arrive at the partial differential equation

$$\boxed{\dot{\eta}_t(\boldsymbol{X}) = -\frac{1}{\Theta_t(\boldsymbol{X})} \mathrm{DIV}[\boldsymbol{Q}_t(\boldsymbol{X})] + \frac{D_t^{\text{int}}(\boldsymbol{X})}{\Theta_t(\boldsymbol{X})}} \tag{9}$$

for all points $\boldsymbol{X} \in \mathscr{B}_0$.

1.6 The constitutive equations

According to Eq. (7), the temperature evolution is restricted by the condition $\dot{\eta}_t \geqslant 0$. This postulate can be satisfied by a non-negative dissipation D_t^{con} arising from conduction of heat, and a non-negative internal dissipation D_t^{int}. The condition $D_t^{\text{con}} \geqslant 0$ is satisfied, for example, by Fourier's law of isotropic heat conduction, defining the components of the Piola-Kirchhoff heat flux vector as

$$[\boldsymbol{Q}_t(\boldsymbol{X})]^A = -k_0 \, J_t(\boldsymbol{X}) \, [\boldsymbol{C}_t^{-1}(\boldsymbol{X})]^{AB} [\nabla \Theta_t(\boldsymbol{X})]_B \doteq -[\boldsymbol{K}_t(\boldsymbol{X})]^{AB} [\nabla \Theta_t(\boldsymbol{X})]_B \tag{10}$$

where $k_0 \in \mathbb{R}_+$ denotes the conductivity in $\mathscr{B}_0$. The dissipation D_t^{con} is thus given as a positive-definite quadratic form with respect to the isotropic Lagrangian conductivity tensor $\boldsymbol{K}_t(\boldsymbol{X})$. The condition $D_t^{\text{int}} \geqslant 0$ has to be satisfied by the constitutive equation for the non-equilibrium stress tensor $\boldsymbol{\Upsilon}_t(\boldsymbol{X})$. We derive this equation by using the balance of thermal energy. In combination with the balance of mechanical energy, we arrive at the equation

$$\int_{\mathscr{B}_0} [\dot{\boldsymbol{\pi}}_t(\boldsymbol{X})]_a \, [\boldsymbol{v}_t(\boldsymbol{X})]^a + \dot{e}_t(\boldsymbol{X}) = \int_{\partial\mathscr{B}_0} [\boldsymbol{v}_t^*(\boldsymbol{X})]_a \, [\boldsymbol{t}_t(\boldsymbol{X})]^a - \int_{\partial\mathscr{B}_0} [\boldsymbol{N}_0(\boldsymbol{X})]_A \, [\boldsymbol{Q}_t(\boldsymbol{X})]^A \tag{11}$$

where the mapping $e_t : \mathscr{B}_0 \rightarrow \mathbb{R}$ denotes the internal energy density. We recall that the term $-[\boldsymbol{N}_0(\boldsymbol{X})]_A \, [\boldsymbol{Q}_t(\boldsymbol{X})]^A$ defines the normal inward heat flux $Q_t(\boldsymbol{X})$. We apply to this boundary integrals Gauss' divergence theorem, and employ the Piola-Kirchhoff theorem. In the end, we obtain by using the localisation theorem the Clausius-Planck inequality

$$D_t^{\text{int}}(\boldsymbol{X}) = \Theta_t(\boldsymbol{X}) \, \dot{\eta}_t(\boldsymbol{X}) - \dot{e}_t(\boldsymbol{X}) + p_t^{\text{int}}(\boldsymbol{X}) \geqslant 0 \tag{12}$$

We let the internal energy density $e_t(\boldsymbol{X})$ be given in dependence of the entropy $\eta_t(\boldsymbol{X})$. Then, we define the internal energy density as the Legendre transform of the free energy $\Psi(\boldsymbol{\Lambda}_t(\boldsymbol{X}))$ with respect to the temperature $\Theta_t(\boldsymbol{X})$. Taking Eq. (3) into account, the Clausius-Planck inequality leads to the internal dissipation

$$D_t^{\text{int}}(\boldsymbol{X}) = [\,\boldsymbol{\Upsilon}_t(\boldsymbol{X})]^{AB} \, [\dot{\boldsymbol{\Gamma}}_t(\boldsymbol{X})]_{AB} = \frac{1}{2} \, [\boldsymbol{M}_t(\boldsymbol{X})]^A{}_B \, [\dot{\boldsymbol{\Gamma}}_t(\boldsymbol{X})]_{AC} [\boldsymbol{\Gamma}_t^{-1}(\boldsymbol{X})]^{CB} \geqslant 0 \tag{13}$$

where $\boldsymbol{M}_t(\boldsymbol{X})$ denotes a mixed-variant stress tensor. Characteristic for a viscoelastic material is a closed stress-strain hysteresis loop during a cyclic loading. The surface area of this loop is proportional to a non-equilibrium strain rate. Since the surface area indicates the energy loss during the deformation, we arrive at a non-equilibrium strain rate dependent internal dissipation. This material behaviour can be obtained by introducing a viscosity. We obtain

$$[\boldsymbol{M}_t(\boldsymbol{X})]^A{}_B = \frac{1}{2}\, V^A{}_B{}^C{}_D\; [\dot{\boldsymbol{\Gamma}}_t(\boldsymbol{X})]_{CE}[\boldsymbol{\Gamma}_t^{-1}(\boldsymbol{X})]^{ED} \tag{14}$$

where the real numbers $V^A{}_B{}^C{}_D = V^C{}_D{}^A{}_B$ designates the entries of the viscosity tensor. The symmetry properties arise from the view of the viscosity as a symmetric positive-definite bilinear form to fulfil the Clausius-Planck inequality. The assumed stress tensor in Eq. (14) has to coincide with the definition of this stress tensor in Eq. (13). This condition leads to the ordinary differential equation

$$\boxed{[\boldsymbol{\Upsilon}_t(\boldsymbol{X})]^{AF} = \frac{1}{4}\,[\boldsymbol{\Gamma}_t^{-1}(\boldsymbol{X})]^{FB}\; V^A{}_B{}^C{}_D\; [\dot{\boldsymbol{\Gamma}}_t(\boldsymbol{X})]_{CE}[\boldsymbol{\Gamma}_t^{-1}(\boldsymbol{X})]^{ED}} \tag{15}$$

determining the time evolution of the internal variable $\boldsymbol{\Gamma}_t(\boldsymbol{X})$, at each point $\boldsymbol{X} \in \mathscr{B}_0$. Taking into account Eq. (13) for the internal dissipation, and Eq. (14) for the mixed-variant stress tensor, the Clausius-Planck inequality can be written as

$$D_t^{\text{int}}(\boldsymbol{X}) = \frac{1}{4}\,[\dot{\boldsymbol{\Gamma}}_t(\boldsymbol{X})]_{AF}[\boldsymbol{\Gamma}_t^{-1}(\boldsymbol{X})]^{FB}\; V^A{}_B{}^C{}_D\; [\dot{\boldsymbol{\Gamma}}_t(\boldsymbol{X})]_{CE}[\boldsymbol{\Gamma}_t^{-1}(\boldsymbol{X})]^{ED} \geqslant 0 \tag{16}$$

The internal dissipation is thus given by a positive-definite quadratic form with respect to the strain rate tensor.

2 THE STRONG FORM OF THE INITIAL BOUNDARY VALUE PROBLEM

We derived a system of differential equations consisting of the Eqs. (6), Eq. (9) and Eq. (15) for the deformation and the deformation velocity, as well as the temperature field and the internal variable field. The Eqs. (6) and Eq. (9) are supplemented by mechanical and thermal boundary conditions, respectively. For both boundary conditions, we assume that $\partial\mathscr{B}_0$ is divided into two disjoint parts. We define the mechanical boundary conditions

$$\begin{aligned} \boldsymbol{\varphi}_t(\boldsymbol{X}) &= \boldsymbol{X} && \text{for all} \quad (t,\boldsymbol{X}) \in \mathscr{T} \times \partial_\varphi\mathscr{B}_0 \\ \boldsymbol{t}_t(\boldsymbol{X}) &= \bar{\boldsymbol{t}}_t(\boldsymbol{X}) && \text{for all} \quad (t,\boldsymbol{X}) \in \mathscr{T} \times \partial_T\mathscr{B}_0 = \mathscr{T} \times (\partial\mathscr{B}_0 \setminus \partial_\varphi\mathscr{B}_0) \end{aligned} \tag{17}$$

specifying the deformation $\boldsymbol{\varphi}_t(\boldsymbol{X})$ and the Piola-Kirchhoff traction vector $\boldsymbol{t}_t(\boldsymbol{X})$ for all points on the corresponding boundaries. In analogy, we assume the following thermal boundary conditions, which prescribe the body temperature $\Theta_t(\boldsymbol{X})$ and the Piola-Kirchhoff heat flux $\boldsymbol{Q}_t(\boldsymbol{X})$ on the corresponding boundaries. We state the conditions

$$\begin{aligned} \Theta_t(\boldsymbol{X}) &= \Theta_\infty && \text{for all} \quad (t,\boldsymbol{X}) \in \mathscr{T} \times \partial_\Theta\mathscr{B}_0 \\ \boldsymbol{Q}_t(\boldsymbol{X}) &= \overline{\boldsymbol{Q}}_t(\boldsymbol{X}) && \text{for all} \quad (t,\boldsymbol{X}) \in \mathscr{T} \times \partial_Q\mathscr{B}_0 = \mathscr{T} \times (\partial\mathscr{B}_0 \setminus \partial_\Theta\mathscr{B}_0) \end{aligned} \tag{18}$$

The differential equations are also related with initial conditions for the motion $\boldsymbol{\varphi}(t)$ and the deformation velocity curve $\boldsymbol{v}(t)$, as well as the temperature evolution curve $\Theta(t)$ and the internal variable evolution curve $\boldsymbol{\Gamma}(t)$. Along with these initial conditions, we arrive at an initial boundary value problem for $\boldsymbol{\varphi}_t$, $\boldsymbol{v}_t$ and Θ_t, however, we obtain an initial value problem for the viscous internal variable field $\boldsymbol{\Gamma}_t$. We assume

$$\begin{aligned} \boldsymbol{\varphi}_{t_0}(\boldsymbol{X}) &= \boldsymbol{X} && \text{and} \quad \Theta_{t_0}(\boldsymbol{X}) = \Theta_0(\boldsymbol{X}) \\ \boldsymbol{v}_{t_0}(\boldsymbol{X}) &= \boldsymbol{v}_0(\boldsymbol{X}) && \text{and} \quad [\boldsymbol{\Gamma}_{t_0}(\boldsymbol{X})]_{AB} = \delta_{AB} \end{aligned} \tag{19}$$

for all points $\boldsymbol{X} \in \mathscr{B}_0$. The initial condition for the viscous evolution equation arises from defining the initial state at $t = 0$ as equilibrium state of the viscous evolution. That means, the free energy $\Psi(\boldsymbol{\Lambda}_t(\boldsymbol{X}))$ coincides with the free energy $\Psi(\Theta_t(\boldsymbol{X}), \boldsymbol{C}_t(\boldsymbol{X}))$ of a thermo-elastic material. For all points $\boldsymbol{X} \in \mathscr{B}_0$, the initial conditions

$$\boldsymbol{\pi}_{t_0}(\boldsymbol{X}) \quad = \quad \rho_0(\boldsymbol{X})\, \boldsymbol{v}_0(\boldsymbol{X}) \qquad\qquad \eta_{t_0}(\boldsymbol{X}) \quad = \quad -\frac{\partial \Psi(\boldsymbol{I}^*, \boldsymbol{I}^*, \Theta_0(\boldsymbol{X}))}{\partial \Theta} \tag{20}$$

specify the momentum evolution and the entropy evolution, where the mapping $\boldsymbol{I}^*$ denotes the identity tensor with the entries δ_{AB}.

2.1 The conservation laws

Let given a pure traction boundary value problem corresponding to $\partial_\varphi \mathscr{B}_0 = \emptyset$ under equilibrated external loads $\bar{\boldsymbol{t}}_t(\boldsymbol{X}) = \boldsymbol{o}$ for all points $\boldsymbol{X} \in \partial_T \mathscr{B}_0$ at any time $t \in \mathscr{T}$. The evolution equations of the initial boundary value problem yields conservation of the total linear momentum function

$$\mathcal{L}(t) = \int_{\mathscr{B}_0} [\boldsymbol{\pi}_t(\boldsymbol{X})]_a \, [\boldsymbol{\xi}_0]^a \tag{21}$$

about the origin of ambient space $\mathscr{A}$. The vector $\boldsymbol{\xi}_0$ denotes a fixed direction vector of a virtual translation of the body in the ambient space at fixed time $t \in \mathscr{T}$. Writing this virtual translation as a curve, the vector $\boldsymbol{\xi}_0$ represents a tangent vector at this curve. By using the fundamental theorem of calculus on the total linear momentum function, we obtain the identity

$$\mathcal{L}(T) - \mathcal{L}(t_0) \doteq \int_{\mathscr{T}} \dot{\mathcal{L}}(t) = \int_{\mathscr{T}} \int_{\mathscr{B}_0} [\dot{\boldsymbol{\pi}}_t(\boldsymbol{X})]_a \, [\boldsymbol{\xi}_0]^a = \int_{\mathscr{B}_0} \big[[\boldsymbol{P}_t^T(\boldsymbol{X})]^{Aa} [\boldsymbol{\xi}_0^*]_a \big]_{,A} \tag{22}$$

where we have employed Eq. (6.2) in the righthand side of this equation for each point $\boldsymbol{X} \in \mathscr{B}_0$. The vector $\boldsymbol{\xi}_0^*$ designates the cotangent vector at the virtual translation curve. With regarding to the assumed vanishing loads $\bar{\boldsymbol{t}}_t(\boldsymbol{X})$ for each $\boldsymbol{X} \in \partial_T \mathscr{B}_0$ at all times $t \in \mathscr{T}$, and using Gauss' divergence theorem together with the Piola-Kirchhoff theorem, the Eqs. (17) lead to

$$\boxed{\mathcal{L}(T) - \mathcal{L}(t_0) = \int_{\mathscr{T}} \int_{\partial_T \mathscr{B}_0} [\boldsymbol{\xi}_0^*]_a \, [\bar{\boldsymbol{t}}_t(\boldsymbol{X})]^a = 0} \tag{23}$$

Thus, we arrive at conservation of the total linear momentum function for any fixed tangent vector $\boldsymbol{\xi}_0$ at the virtual translation curve. The evolution equations of the initial boundary value problem have the total angular momentum function $\mathcal{J}(t)$ as a second first integral about the origin of the ambient space. This function is defined by

$$\mathcal{J}(t) = \int_{\mathscr{B}_0} \epsilon_{abc} \delta^{cd} \, [\boldsymbol{\varphi}_t(\boldsymbol{X})]^b \, [\boldsymbol{\pi}_t(\boldsymbol{X})]_d [\boldsymbol{\xi}_0]^a \tag{24}$$

where ϵ_{abc} denotes the permutation or Levi-Civita symbol. In Eq. (24), the vector $\boldsymbol{\xi}_0$ represents a fixed axial vector, that is the direction vector of a rotation axis, associated with an arbitrary virtual rotation of the body around the origin of $\mathscr{A}$ at fixed time $t \in \mathscr{T}$. The circular curve $\boldsymbol{\varphi}_t(\boldsymbol{X})(s)$ pertaining to this virtual rotation of the point $\boldsymbol{X} \in \mathscr{B}_0$ has a tangent vector

$$[\boldsymbol{\nu}_t(\boldsymbol{X})]^a = \delta^{ab} \epsilon_{bcd} \, [\boldsymbol{\xi}_0]^c \, [\boldsymbol{\varphi}_t(\boldsymbol{X})(s)]^d = [\hat{\boldsymbol{\xi}}_0]^a{}_d \, [\boldsymbol{\varphi}_t(\boldsymbol{X})(s)]^d \tag{25}$$

The mapping $\hat{\boldsymbol{\xi}}_0$ denotes the spin tensor associated with the axial vector $\boldsymbol{\xi}_0$. We are able to verify that the total angular momentum function is a constant of the motion by stating the fundamental theorem of calculus

$$\mathcal{J}(T) - \mathcal{J}(t_0) = \int_{\mathscr{T}} \int_{\mathscr{B}_0} \epsilon_{abc}\delta^{cd} \, [\dot{\boldsymbol{\varphi}}_t(\boldsymbol{X})]^b \, [\boldsymbol{\pi}_t]_d \, [\boldsymbol{\xi}_0]^a + \epsilon_{abc}\delta^{cd} \, [\boldsymbol{\varphi}_t(\boldsymbol{X})]^b \, [\dot{\boldsymbol{\pi}}_t]_d \, [\boldsymbol{\xi}_0]^a \tag{26}$$

Employing the Eqs. (6), and recalling the definition of the conjugated momentum, the first term on the righthand side vanishes due to the skew-symmetry of the permutation symbol. We rewrite the second term by using the product rule of partial differentiation with respect to the point $\boldsymbol{X} \in \mathscr{B}_0$, which provides two subterms, of which the first vanish, according to the symmetry of the Kirchhoff stress tensor

$$[\boldsymbol{\tau}_t(\boldsymbol{X})]^{ab} = [\boldsymbol{F}_t(\boldsymbol{X})]^a{}_A \, [\boldsymbol{S}_t(\boldsymbol{X})]^{AB} \, [\boldsymbol{F}_t^T(\boldsymbol{X})]_B{}^b \tag{27}$$

in conjunction with the skew-symmetry of the permutation symbol. To the second subterm, we apply Gauss' divergence theorem, and employ the Piola-Kirchhoff traction vector, according to the Piola-Kirchhoff theorem. Then, Eq. (17) leads to

$$\boxed{\mathcal{J}(T) - \mathcal{J}(t_0) = \int_{\mathscr{T}} \int_{\partial_T \mathscr{B}_0} [\boldsymbol{\nu}_t^*(\boldsymbol{X})]_a \, [\bar{\boldsymbol{t}}_t(\boldsymbol{X})]^a = 0} \tag{28}$$

where the vector $\boldsymbol{\nu}_t^*(\boldsymbol{X}) \in T_x^* \mathscr{B}_t$ denotes the cotangent vector at the virtual rotation curve. Since the assumed loads vanish for each $\boldsymbol{X} \in \partial_T \mathscr{B}_0$ on the traction boundary at all times $t \in \mathscr{T}$, we obtain conservation of the total angular momentum function for the time interval $\mathscr{T}$.

2.2 The a priori stability estimate

The equilibrium state of the body is a fix point of its time evolution equations. If there exists a corresponding Lyapunov function, this equilibrium is called stable. Therefore, stability of nonlinear equilibria is often phrased in terms of an a priori estimate arising from an existent Lyapunov function. Again, we assume equilibrated mechanical loads associated with a thermal Neumann boundary $\partial_Q \mathscr{B}_0 = \emptyset$. We define the function

$$\mathcal{V}(t) = \mathcal{T}(t) + \int_{\mathscr{B}_0} \eta_t(\boldsymbol{X}) \, \vartheta_t(\boldsymbol{X}) + \Psi(\Theta_t(\boldsymbol{X}), \boldsymbol{C}_t(\boldsymbol{X}), \boldsymbol{\Gamma}_t(\boldsymbol{X})) = \mathcal{T}(t) + \hat{\mathcal{E}}(t) \tag{29}$$

and show that it is a Lyapunov function. Considering in this Lyapunov function the tangent vector $\vartheta_t(\boldsymbol{X})$ as well as a free energy $\Psi(\boldsymbol{\Lambda}_t(\boldsymbol{X}))$, vanishing at environment temperature, we ensure the equilibrium state at environment temperature. Application of the fundamental theorem of calculus provides the equation

$$\mathcal{V}(T) - \mathcal{V}(t_0) = \int_{\mathscr{T}} \int_{\mathscr{B}_0} [\dot{\boldsymbol{\pi}}_t(\boldsymbol{X})]_a \, [\boldsymbol{v}_t(\boldsymbol{X})]^a + \dot{\eta}_t(\boldsymbol{X}) \, \vartheta_t(\boldsymbol{X}) + \eta_t(\boldsymbol{X}) \, \dot{\Theta}_t(\boldsymbol{X}) + \dot{\Psi}(\boldsymbol{X}) \tag{30}$$

where in the first term of Eq. (30) the definition of the conjugated momentum has been taken into account. Now, we employ the Eqs. (6) in the first term, and bear in mind the product rule of partial differentiation with respect to a point $\boldsymbol{X} \in \mathscr{B}_0$. In this way, we obtain

$$\int_{\mathscr{B}_0} [\dot{\boldsymbol{\pi}}_t(\boldsymbol{X})]_a \, [\boldsymbol{v}_t(\boldsymbol{X})]^a = \int_{\partial_T \mathscr{B}_0} [\boldsymbol{v}_t^*(\boldsymbol{X})]_a \, [\bar{\boldsymbol{t}}_t(\boldsymbol{X})]^a - \mathcal{P}^{\text{int}}(t) \tag{31}$$

after applying Gauss' divergence theorem and the Piola-Kirchhoff theorem, as well as Eq. (17) to the volume integral. According to the absence of loads, the first term of this equation vanish. Since terms associated with the stress power annihilate each other, and likewise the terms with the time derivative of the temperature, we arrive at the balance equation

$$\mathcal{V}(T) - \mathcal{V}(t_0) = \int_{\mathscr{T}}\int_{\mathscr{B}_0} \dot{\eta}_t(\boldsymbol{X})\,\vartheta_t(\boldsymbol{X}) - [\,\boldsymbol{\Upsilon}_t(\boldsymbol{X})]^{AB}\,[\dot{\boldsymbol{\Gamma}}(\boldsymbol{X})]_{AB} \tag{32}$$

Now, we employ Eq. (9) in the first term on the righthand side of Eq. (32). Using again the product rule of partial differentiation, we obtain a volume integral, which can be transformed into a boundary integral by applying Gauss' divergence theorem. Then, we employ the Piola-Kirchhoff heat flux, given by Eq. (18), in this boundary integral, and arrive at the expression

$$-\int_{\mathscr{B}_0} \frac{\Theta_\infty}{\Theta_t(\boldsymbol{X})}\,D_t^{\mathrm{tot}}(\boldsymbol{X}) + \int_{\mathscr{B}_0} D_t^{\mathrm{int}}(\boldsymbol{X}) - \int_{\partial_Q\mathscr{B}_0} \frac{\vartheta_t(\boldsymbol{X})}{\Theta_t(\boldsymbol{X})}\,[\boldsymbol{N}_0(\boldsymbol{X})]_A\,[\overline{\boldsymbol{Q}}_t(\boldsymbol{X})]^A \tag{33}$$

The boundary integral in this term vanish, due to the empty thermal Neumann boundary $\partial_Q\mathscr{B}_0$. Finally, we introduce in the last term of Eq. (32) the evolution equation for the viscous internal variable. According to Eq. (16), this term coincides with the negative internal dissipation. In the end, we get at the stability estimate

$$\boxed{\mathcal{V}(T) - \mathcal{V}(t_0) = -\int_{\mathscr{T}}\int_{\mathscr{B}_0} \frac{\Theta_\infty}{\Theta_t(\boldsymbol{X})}\,D_t^{\mathrm{tot}}(\boldsymbol{X}) \leqslant 0} \tag{34}$$

for the time evolution of the considered continuum body during the time interval $\mathscr{T}$ of interest. Note that the Lyapunov function describes the relative total energy of the body about Θ_∞.

3 THE WEAK FORM OF THE INITIAL BOUNDARY VALUE PROBLEM

We deduce the weak forms directly from the defined Lyapunov function. In this way, we obtain the convenient Galerkin method in order to satisfy Eq. (34). We begin by determining the directional derivative along the continuous time curve $\gamma_t(s) = \mathcal{T}(t+s)$. Then, the fundamental theorem of calculus yields

$$\mathcal{T}(T) - \mathcal{T}(t_0^+) = \int_{\mathscr{T}}\int_{\mathscr{B}_0} [\dot{\boldsymbol{\pi}}_t(\boldsymbol{X})]_a\,[\boldsymbol{v}_t(\boldsymbol{X})]^a \tag{35}$$

where

$$\mathcal{T}(t_0^+) = \lim_{s\to 0^+} \mathcal{T}(t_0+s) \qquad \text{and} \qquad \mathcal{T}(T) = \lim_{s\to 0^+} \mathcal{T}(T-s) \tag{36}$$

denote the kinetic energies at the lower bound and at the upper bound of the time curve, respectively. Note that at any time $t \in \mathscr{T}$ the field $\dot{\boldsymbol{\pi}}_t$ is tangent to the continuous variation curve $\boldsymbol{\gamma}_t(s) = \boldsymbol{\pi}_{t+s}$ in the cotangent space of the motion. Hence, the tangent vector field $\dot{\boldsymbol{\pi}}_t$ represents an admissible test function for a weak form of Eq. (6.1). We employ this equation in the righthand side of Eq. (35), and obtain the identity

$$\int_{\mathscr{T}}\int_{\mathscr{B}_0} [\dot{\boldsymbol{\pi}}_t(\boldsymbol{X})]_a\,[\boldsymbol{v}_t(\boldsymbol{X})]^a = \int_{\mathscr{T}}\int_{\mathscr{B}_0} [\dot{\boldsymbol{\pi}}_t(\boldsymbol{X})]_a\,[\dot{\boldsymbol{\varphi}}_t(\boldsymbol{X})]^a \tag{37}$$

The time displacement $\boldsymbol{\gamma}_t(s) = \boldsymbol{\pi}_{t+s}$ satisfies the vanishing conjugated momentum at the time-independent Dirichlet boundary, and lead to vanishing tangent vectors on $\partial_\varphi\mathscr{B}_0$. A fixed lower bound of this curve at initial time t_0 also leads to a zero tangent vector. Consequently, the initial condition of the motion can be fulfilled exactly. We obtain the weak form

$$\boxed{\int_{\mathscr{T}}\int_{\mathscr{B}_0}[\delta\dot{\boldsymbol{\pi}}_t(\boldsymbol{X})]_a\,[\dot{\boldsymbol{\varphi}}_t(\boldsymbol{X})]^a = \int_{\mathscr{T}}\int_{\mathscr{B}_0}[\delta\dot{\boldsymbol{\pi}}_t(\boldsymbol{X})]_a\,[\boldsymbol{v}_t(\boldsymbol{X})]^a} \tag{38}$$

Hence, we apply a cG method in time (cp. Ref. [1] and references therein). Given any time $t\in\mathscr{T}$, the vector field $\dot{\boldsymbol{\varphi}}_t$ is tangent to the continuous curve $\boldsymbol{\gamma}_t(s)=\boldsymbol{\varphi}_{t+s}$ of deformations. Therefore, this field is an admissible test function for a weak form of Eq. (6.2). We employ Eq. (6.2) in the righthand side of Eq. (37), integrate by part and subsequently apply Gauss' divergence theorem. Noticing the Piola-Kirchhoff theorem and the mechanical boundary conditions, we get at

$$\int_{\mathscr{T}}\int_{\mathscr{B}_0}[\dot{\boldsymbol{\pi}}_t(\boldsymbol{X})]_a\,[\dot{\boldsymbol{\varphi}}_t(\boldsymbol{X})]^a = \int_{\mathscr{T}}\int_{\partial_T\mathscr{B}_0}[\bar{\boldsymbol{t}}^*_t(\boldsymbol{X})]_a\,[\dot{\boldsymbol{\varphi}}_t(\boldsymbol{X})]^a - \int_{\mathscr{T}}\int_{\mathscr{B}_0}[\boldsymbol{P}^*_t(\boldsymbol{X})]_a{}^A\,[\dot{\boldsymbol{\varphi}}_t(\boldsymbol{X})]^a{}_{,A} \tag{39}$$

The variation curve $\boldsymbol{\gamma}_t(s)=\boldsymbol{\varphi}_{t+s}$ satisfies the time-independent Dirichlet boundary condition of the motion, and lead to vanishing tangent vectors on the boundary $\partial_\varphi\mathscr{B}_0$. Since the tangent vector at a fixed lower bound $\boldsymbol{X}$ of this curve vanish, the initial condition of the conjugated momentum can be fulfilled exactly. In this way, we obtain

$$\boxed{\begin{aligned}&\int_{\mathscr{T}}\int_{\mathscr{B}_0}[\dot{\boldsymbol{\pi}}_t(\boldsymbol{X})]_a\,[\delta\dot{\boldsymbol{\varphi}}_t(\boldsymbol{X})]^a = \\ &\qquad\int_{\mathscr{T}}\int_{\partial_T\mathscr{B}_0}[\bar{\boldsymbol{t}}^*_t(\boldsymbol{X})]_a\,[\delta\dot{\boldsymbol{\varphi}}_t(\boldsymbol{X})]^a - \int_{\mathscr{T}}\int_{\mathscr{B}_0}[\boldsymbol{P}^*_t(\boldsymbol{X})]_a{}^A\,[\delta\dot{\boldsymbol{\varphi}}_t(\boldsymbol{X})]^a{}_{,A}\end{aligned}} \tag{40}$$

Thus, we determine a continuous weak time evolution $\boldsymbol{\pi}$ of the conjugated momentum as well as a continuous weak motion $\boldsymbol{\varphi}$, wherefore the initial kinetic energy $\mathcal{T}(t_0)$, and the kinetic energy $\mathcal{T}(t_0^+)$ at the lower bound of the time curve coincides. Nevertheless, the time evolution $\boldsymbol{P}^*$ of the covariant first Piola-Kirchhoff stress tensor field is, in general, only related with the lower bound of the continuous curve $\gamma_t(s)=\boldsymbol{P}^*_{t_0+s}$. We obtain the kinetic energy balance

$$\mathcal{T}(T)-\mathcal{T}(t_0) = \int_{\mathscr{T}}\int_{\partial_T\mathscr{B}_0}[\bar{\boldsymbol{t}}^*_t(\boldsymbol{X})]_a\,[\dot{\boldsymbol{\varphi}}_t(\boldsymbol{X})]^a - \int_{\mathscr{T}}\int_{\mathscr{B}_0}[\boldsymbol{P}^*_t(\boldsymbol{X})]_a{}^A\,[\dot{\boldsymbol{F}}_t(\boldsymbol{X})]^a{}_A \tag{41}$$

As next step, we consider the second part of Eq. (29), that is the relative internal energy $\hat{\mathcal{E}}:\mathscr{T}\to\mathbb{R}$ of the body. We calculate the directional derivative along the continuous time curve $\gamma_t(s)=\hat{\mathcal{E}}(t+s)$, and apply the fundamental theorem of calculus. We denote by $\hat{\mathcal{E}}(t_0^+)$ the energy at the lower bound of the time curve, and $\hat{\mathcal{E}}(T)$ designates the energy at the upper bound. We obtain the balance

$$\hat{\mathcal{E}}(T)-\hat{\mathcal{E}}(t_0^+) = \int_{\mathscr{T}}\int_{\mathscr{B}_0}\dot{\eta}_t(\boldsymbol{X})\,\vartheta_t(\boldsymbol{X}) + [\boldsymbol{P}^*_t(\boldsymbol{X})]_a{}^A\,[\dot{\boldsymbol{F}}_t(\boldsymbol{X})]^a{}_A - [\boldsymbol{\varUpsilon}_t(\boldsymbol{X})]^{AB}\,[\dot{\boldsymbol{\varGamma}}_t(\boldsymbol{X})]_{AB} \tag{42}$$

The relative temperature field ϑ_t is tangent to the variation curve $\gamma_t(s)=\Theta_t+s\,\vartheta_t$ through the fixed temperature field Θ_t for any time $t\in\mathscr{T}$. Hence, the relative temperature field is an admissible test function for a weak form of Eq. (9). We combine this equation with the first term on the righthand side of Eq. (42), and get at the identity

$$\begin{aligned}\int_{\mathscr{T}}\int_{\mathscr{B}_0}\dot{\eta}_t(\boldsymbol{X})\,\vartheta_t(\boldsymbol{X}) = &-\int_{\mathscr{T}}\int_{\partial_Q\mathscr{B}_0}\frac{\vartheta_t(\boldsymbol{X})}{\Theta_t(\boldsymbol{X})}\,[\boldsymbol{N}_0(\boldsymbol{X})]_A\,[\overline{\boldsymbol{Q}}_t(\boldsymbol{X})]^A + \\ &+\int_{\mathscr{T}}\int_{\mathscr{B}_0}\frac{\Theta_\infty}{\Theta_t(\boldsymbol{X})}\,[\vartheta_t(\boldsymbol{X})]_{,A}\,[\boldsymbol{H}_t(\boldsymbol{X})]^A + \frac{\vartheta_t(\boldsymbol{X})}{\Theta_t(\boldsymbol{X})}\,D^{\mathrm{int}}_t(\boldsymbol{X})\end{aligned} \tag{43}$$

The variation curve $\gamma_t(s) = \Theta_t + s\,\vartheta_t$ bear in mind the fixed environment temperature Θ_∞ at the thermal Dirichlet boundary. Since the relative temperature field ϑ_t vanish solely at the boundary $\partial_\Theta \mathscr{B}_0$ at any time $t \in \mathscr{T}$, the lower bound $\gamma_{t_0}(s)$ of this continuous variation curve is, in general, varied. The lower bound therefore differs from the initial values $\Theta_0(\boldsymbol{X})$ for any points $\boldsymbol{X} \in \mathscr{B}_0$, and we obtain a jump

$$[\![\Theta_{t_0}]\!] = \Theta_{t_0} - \Theta_0 \tag{44}$$

in the temperature time evolution at initial time t_0. According to the definition of the entropy field, we also get a jump $[\![\eta_{t_0}]\!]$ in the entropy evolution. Thus, the energy $\hat{\mathcal{E}}(t_0^+)$ differs from the initial value $\hat{\mathcal{E}}(t_0)$ of the relative internal energy. However, we arrive at the energy difference between the upper bound $\hat{\mathcal{E}}(T)$ and the initial value $\hat{\mathcal{E}}(t_0)$ by introducing the energy $\hat{\mathcal{E}}(t_0)$ in Eq. (42). In this way, we obtain the balance equation

$$\hat{\mathcal{E}}(T) - \hat{\mathcal{E}}(t_0) = \hat{\mathcal{E}}(T) - \hat{\mathcal{E}}(t_0^+) + \hat{\mathcal{E}}(t_0^+) - \hat{\mathcal{E}}(t_0) = \left[\!\!\left[\hat{\mathcal{E}}(t_0)\right]\!\!\right] + \hat{\mathcal{E}}(T) - \hat{\mathcal{E}}(t_0^+) \tag{45}$$

In order to get at Eq. (34), we have to assume a vanishing Piola-Kirchhoff traction vector field $\bar{\boldsymbol{t}}_t$ on the mechanical Neumann boundary. Consequently, addition of Eq. (41) for the continuous time course of the kinetic energy, and Eq. (45) pertaining to the discontinuous time evolution of the relative internal energy leads to the balance equation

$$\mathcal{V}(T) - \mathcal{V}(t_0) = \left[\!\!\left[\hat{\mathcal{E}}(t_0)\right]\!\!\right] + \int_{\mathscr{T}}\int_{\mathscr{B}_0} \dot{\eta}_t(\boldsymbol{X})\,\vartheta_t(\boldsymbol{X}) - [\,\boldsymbol{\Upsilon}_t(\boldsymbol{X})]^{AB}\,[\dot{\boldsymbol{\Gamma}}_t(\boldsymbol{X})]_{AB} \tag{46}$$

because terms associated with the stress power annihilate each other. We deduce from Eq. (46) a weak form of Eq. (9). The corresponding initial condition associated with the temperature is enforced weakly by a so-called trace term, which fulfils Eq. (46). Recall that the density $\hat{e}_t : \mathscr{B}_0 \rightarrow \mathbb{R}$ of the relative internal energy is defined by the expression

$$\hat{e}_t(\boldsymbol{X}) = \eta_t(\boldsymbol{X})\,\vartheta_t(\boldsymbol{X}) + \Psi(\boldsymbol{\Gamma}_t(\boldsymbol{X}), \boldsymbol{C}_t(\boldsymbol{X}), \Theta_t(\boldsymbol{X})) \tag{47}$$

The energy jump in Eq. (46) then leads to a jump $[\![\hat{e}_{t_0}(\boldsymbol{X})]\!]$ in the density for all points $\boldsymbol{X} \in \mathscr{B}_0$. We assume that this jump coincides with the trace term $\vartheta_{t_0}(\boldsymbol{X})\,\hat{\eta}_{t_0}(\boldsymbol{X})$, where $\hat{\eta}_{t_0}(\boldsymbol{X})$ is a unknown entropy trace. We search for the smallest entropy trace, which fulfils this constraint. Hence, we search for a trace $\hat{\eta}_{t_0}(\boldsymbol{X})$, which minimise the Lagrange function

$$F(\hat{\eta}_{t_0}(\boldsymbol{X}), \lambda(\boldsymbol{X})) = \frac{1}{2}\,\hat{\eta}_{t_0}^2(\boldsymbol{X}) + \lambda(\boldsymbol{X})\,\{\vartheta_{t_0}(\boldsymbol{X})\,\hat{\eta}_{t_0}(\boldsymbol{X}) - [\![\hat{e}_{t_0}(\boldsymbol{X})]\!]\} \tag{48}$$

where $\lambda(\boldsymbol{X})$ denotes the Lagrange multiplier. According to the Euler-Lagrange equation corresponding to the entropy trace, $\hat{\eta}_{t_0}(\boldsymbol{X})$ coincides with $-\lambda(\boldsymbol{X})\,\vartheta_{t_0}(\boldsymbol{X})$. Employing this relation in the Euler-Lagrange equation corresponding to the Lagrange multiplier, the energy jump term reads

$$\left[\!\!\left[\hat{\mathcal{E}}(t_0)\right]\!\!\right] = \int_{\mathscr{B}_0} [\![\hat{e}_{t_0}(\boldsymbol{X})]\!] = \int_{\mathscr{B}_0} \hat{\eta}_{t_0}(\boldsymbol{X})\,\vartheta_{t_0}(\boldsymbol{X}) = \int_{\mathscr{B}_0} \frac{[\![\hat{e}_{t_0}(\boldsymbol{X})]\!]}{\vartheta_{t_0}(\boldsymbol{X})}\;\vartheta_{t_0}(\boldsymbol{X}) \tag{49}$$

Consider the entropy trace as function of the temperature $\Theta_{t_0}(\boldsymbol{X})$, and apply L'Hôpital's rule. We realise that the limit of this fraction, as $\Theta_{t_0}(\boldsymbol{X})$ approaches Θ_∞, is zero as for the density jump $[\![\hat{e}_{t_0}(\boldsymbol{X})]\!]$ alone. Hence, we have not introduced a singularity in this way. Eq. (46) then reads

$$\mathcal{V}(T) - \mathcal{V}(t_0) = \int_{\mathscr{B}_0} \frac{[\![\hat{e}_{t_0}(\boldsymbol{X})]\!]}{\vartheta_{t_0}(\boldsymbol{X})}\;\vartheta_{t_0}(\boldsymbol{X}) + \int_{\mathscr{T}}\int_{\mathscr{B}_0} \dot{\eta}_t(\boldsymbol{X})\,\vartheta_t(\boldsymbol{X}) - [\,\boldsymbol{\Upsilon}_t(\boldsymbol{X})]^{AB}\,[\dot{\boldsymbol{\Gamma}}_t(\boldsymbol{X})]_{AB} \tag{50}$$

The first and the second term of this equation include the relative Lagrangian temperature field as weighting function. These terms are therefore related to the space-time weak form of the entropy evolution equation. Thus, we obtain the weak form

$$\boxed{\begin{aligned}\int_{\mathscr{B}_0}\frac{[\![\hat{e}_{t_0}(\boldsymbol{X})]\!]}{\vartheta_{t_0}(\boldsymbol{X})}\,\delta\Theta_{t_0}(\boldsymbol{X})+\int_{\mathscr{T}}\int_{\mathscr{B}_0}\dot{\eta}_t(\boldsymbol{X})\,\delta\Theta_t(\boldsymbol{X})=-\int_{\mathscr{T}}\int_{\partial_Q\mathscr{B}_0}\frac{\delta\Theta_t(\boldsymbol{X})}{\Theta_t(\boldsymbol{X})}\,\overline{Q}_t(\boldsymbol{X})+\\+\int_{\mathscr{T}}\int_{\mathscr{B}_0}\frac{\Theta_\infty}{\Theta_t(\boldsymbol{X})}\,[\delta\Theta_t(\boldsymbol{X})]_{,A}\,[\boldsymbol{H}_t(\boldsymbol{X})]^A+\delta\Theta_t(\boldsymbol{X})\,\frac{D_t^{\text{int}}(\boldsymbol{X})}{\Theta_t(\boldsymbol{X})}\end{aligned}} \tag{51}$$

where $\delta\Theta_{t_0}$ varies the temperature field at the limit from above. Accordingly, this weak form leads to a dG method in time (cp. Ref. [5]), which is energy-consistent. According to the empty boundary $\partial_Q\mathscr{B}_0$, associated with Eq. (34), a comparison of Eq. (51) with the first two terms on the righthand side of Eq. (50) yields the balance

$$\mathcal{V}(T)-\mathcal{V}(t_0)=-\int_{\mathscr{T}}\int_{\mathscr{B}_0}\frac{\Theta_\infty}{\Theta_t(\boldsymbol{X})}D_t^{\text{tot}}(\boldsymbol{X})+\int_{\mathscr{T}}\int_{\mathscr{B}_0}D_t^{\text{int}}(\boldsymbol{X})-[\,\boldsymbol{\Upsilon}_t(\boldsymbol{X})]^{AB}\,[\dot{\boldsymbol{\Gamma}}_t(\boldsymbol{X})]_{AB} \tag{52}$$

in which Eq. (8) has been employed. Finally, we deduce a weak form of Eq. (15). Here, we go a different way as for the former time evolution equations. We determine the viscous internal variable at each considered point $\boldsymbol{X}\in\mathscr{B}_0$. That is possible, because the viscous internal variable evolution is only a coupled initial value problem. Employing Eq. (15) in the last term of Eq. (52), for a fixed point $\boldsymbol{X}\in\mathscr{B}_0$, we obtain the temporally weak form

$$\boxed{\begin{aligned}&\int_{\mathscr{T}}[\,\boldsymbol{\Upsilon}(\boldsymbol{X})]^{AF}\,[\delta\dot{\boldsymbol{\Gamma}}_t(\boldsymbol{X})]_{AF}=\\&\qquad\frac{1}{4}\int_{\mathscr{T}}[\delta\dot{\boldsymbol{\Gamma}}_t(\boldsymbol{X})]_{AF}[\boldsymbol{\Gamma}_t^{-1}(\boldsymbol{X})]^{FB}\;V^{A}{}_{B}{}^{C}{}_{D}\;[\dot{\boldsymbol{\Gamma}}_t(\boldsymbol{X})]_{CE}[\boldsymbol{\Gamma}_t^{-1}(\boldsymbol{X})]^{ED}\end{aligned}} \tag{53}$$

wherein the test function is a tangent vector of the variation curve $\gamma_t(\boldsymbol{X})(s)=\boldsymbol{\Gamma}_{t+s}(\boldsymbol{X})$ of the viscous internal variable $\boldsymbol{\Gamma}_t(\boldsymbol{X})$. Since the tangent vector associated with a fixed lower bound of the variation curve at initial time t_0 vanish for all $\boldsymbol{X}\in\mathscr{B}_0$, the initial condition of the internal variable at any point $\boldsymbol{X}\in\mathscr{B}_0$ can be satisfied exactly. Hence, the time evolution of the viscous internal variable is continuous. Eq. (53) leads to the identity

$$\int_{\mathscr{T}}\int_{\mathscr{B}_0}[\,\boldsymbol{\Upsilon}_t(\boldsymbol{X})]^{AF}\,[\dot{\boldsymbol{\Gamma}}_t(\boldsymbol{X})]_{AF}=\int_{\mathscr{T}}\int_{\mathscr{B}_0}D_t^{\text{int}}(\boldsymbol{X}) \tag{54}$$

relating the last term on the righthand side of Eq. (52) to the internal dissipation, given in Eq. (16). Note that Eq. (53) corresponds to a cG method in time at each considered integration point $\boldsymbol{X}\in\mathscr{B}_0$. According to the Eqs. (52) and (54), we arrive at the a priori stability estimate.

4 THE FINITE ELEMENT APPROXIMATION OF THE WEAK FORMS

First, we perform a temporal finite element approximation. This leads to a finite-dimensional approximation of the considered time evolutions. Then, we obtain a finite-dimensional approximation of the Lagrangian fields at fixed time by introducing a spatial finite element approximation.

4.1 The temporal finite element approximation

We introduce a partition of the time interval $\mathscr{T} = [t_0, T]$ into $m_{el} \geqslant 1$ disjoint sub-intervals $\mathscr{T}^n$, $n \in \mathscr{M}_{el} = \{1, \ldots, m_{el}\}$, such that the union of all sub-intervals coincides with $\mathscr{T}$. This partition is related with a mesh $t_0 = t^1 < t^2 < \ldots < t^{m_{el}} < t^{m_{el}+1} = T$ of time points. We refer to a sub-interval $\mathscr{T}^n = [t^n, t^{n+1}]$ as the n-th time element. In order to increase the approximation accuracy, we introduce time nodes $t_i^n < t_k^n \in \mathscr{T}^n$, where $i < k \in \mathscr{M}_{en} = \{1, \ldots, m_{en}\}$ on each time element, which are such that $t_1^n = t^n$ and $t_{m_{en}}^n = t^{n+1}$. The difference $h^n = t_{m_{en}}^n - t_1^n$ is called the time step size. By the transformation

$$\tau^n : \mathscr{I}_\alpha \ni \alpha \mapsto \sum_{i=1}^{m_{en}} M^i(\alpha)\, t_i^n \in \mathscr{T}^n \tag{55}$$

we map a temporal parent domain $\mathscr{I}_\alpha = [0, 1]$ on a time element $\mathscr{T}^n$. The shape functions $M^i : \mathscr{I}_\alpha \to \mathbb{R}$ are Lagrange polynomials, which satisfy $M^i(\alpha_k) = \delta_k{}^i$. Thus, the time nodes $\alpha_k \in \mathscr{I}_\alpha$, $k \in \mathscr{M}_{en}$, in $\mathscr{I}_\alpha$ are mapped to the time nodes $t_k^n = \tau^n(\alpha_k)$ in $\mathscr{T}^n$. Since we restrict ourselves to an equidistant distribution of the time nodes t_k^n, there remains

$$\tau^n(\alpha) = (1 - \alpha)\, t_1^n + \alpha\, t_{m_{en}}^n \tag{56}$$

The partition of $\mathscr{T}$ divides the time integral of a weak form into a sum of m_{el} sub-integrals with respect to the time elements $\mathscr{T}^n$. We get m_{el} coupled systems of weak forms. By using Eq. (56), we transform each time element to the parent domain. For each $n \in \mathscr{M}_{el}$, we obtain the weak form

$$\int_{\mathscr{I}_\alpha}\int_{\mathscr{B}_0} [\delta\dot{\boldsymbol{\pi}}_\alpha^n(\boldsymbol{X})]_a\, [\dot{\boldsymbol{\varphi}}_\alpha^n(\boldsymbol{X})]^a = \int_{\mathscr{I}_\alpha}\int_{\mathscr{B}_0} [\delta\dot{\boldsymbol{\pi}}_\alpha^n(\boldsymbol{X})]_a\, [\boldsymbol{v}_\alpha^n(\boldsymbol{X})]^a \tag{57}$$

where we have used the substitution rule together with the identity $\mathrm{D}\tau^n(\alpha) = h^n$ for relating the time integration to the parent domain. The mapping $\boldsymbol{\varphi}_\alpha^n = \boldsymbol{\varphi}|_{\mathscr{T}^n}(\tau^n(\alpha))$ designates a deformation field at any time point $t = \tau^n(\alpha) \in \mathscr{T}^n$. The field $\boldsymbol{v}_\alpha^n$ denotes the corresponding velocity field. We approximate the corresponding time evolutions, such that

$$\boldsymbol{\varphi}_\alpha^n = \sum_{i=1}^{m_{en}} M^i(\alpha)\, \boldsymbol{\varphi}_{\alpha_i}^n \qquad \text{and} \qquad \boldsymbol{v}_\alpha^n = \sum_{i=1}^{m_{en}} M^i(\alpha)\, \boldsymbol{v}_{\alpha_i}^n \tag{58}$$

Applying the same shape functions as in Eq. (55), we obtain an isoparametric finite element approximation. Since we approximate the deformation and not its time derivative, we have to apply the chain rule of differentiation for calculating the time derivative $\dot{\boldsymbol{\varphi}}_\alpha^n$ on the lefthand side of Eq. (57). The first weak equation of motion on $\mathcal{T}^n$, $n \in \mathscr{M}_{el}$, then, takes the form

$$\boxed{\int_{\mathscr{I}_\alpha}\int_{\mathscr{B}_0} [\delta\dot{\boldsymbol{\pi}}_\alpha^n(\boldsymbol{X})]_a\, [\partial_\alpha\boldsymbol{\varphi}_\alpha^n(\boldsymbol{X})]^a = h^n \int_{\mathscr{I}_\alpha}\int_{\mathscr{B}_0} [\delta\dot{\boldsymbol{\pi}}_\alpha^n(\boldsymbol{X})]_a\, [\boldsymbol{v}_\alpha^n(\boldsymbol{X})]^a} \tag{59}$$

where ∂_α indicates the partial derivative of the motion $\hat{\boldsymbol{\varphi}}|_{\mathscr{T}^n}(\tau^n(\alpha), \boldsymbol{X})$ with respect to α. We approximate the time evolution curve $\delta\dot{\boldsymbol{\pi}}^n$ pertaining to the time derivative $\delta\dot{\boldsymbol{\pi}}_\alpha^n$ of the variation of the conjugated momentum field on $\mathscr{T}_n$ directly on the parent domain. We obtain the definition

$$\delta\dot{\boldsymbol{\pi}}_\alpha^n = \sum_{j=1}^{m_{eq}} \tilde{M}^j(\alpha)\, \delta\dot{\boldsymbol{\pi}}_{\tilde{\alpha}_j}^n \tag{60}$$

Since the variation $\delta\dot{\boldsymbol{\pi}}^n_{\alpha_1}$ at the time node $t^n_1 = \tau^n(\alpha_1)$ vanish, the initial conjugated momentum $\boldsymbol{\pi}_{t^{n-1}_{m_{en}}}$ coincides with $\boldsymbol{\pi}^n_{\alpha_1}$. The shape functions $\tilde{M}^j$, where $j \in \mathscr{M}_{eq} = \{1, \ldots, m_{eq}\}$ denote Lagrange polynomials, satisfying the conditions $\tilde{M}^j(\tilde{\alpha}_l) = \delta_l{}^j$, $j, l \in \mathscr{M}_{eq}$. The points $\tilde{\alpha}_l$ designate temporal test notes on the parent domain. The number m_{eq} of these test notes coincides with $m_{en} - 1$. According to Eq. (40), we obtain for each element $\mathcal{T}^n$, $n \in \mathscr{M}_{el}$, the weak form

$$\boxed{\begin{aligned}&\int_{\mathscr{I}_\alpha}\int_{\mathscr{B}_0} [\partial_\alpha \boldsymbol{\pi}^n_\alpha(\boldsymbol{X})]_a\, [\delta\dot{\boldsymbol{\varphi}}^n_\alpha(\boldsymbol{X})]^a = \\ &\qquad h^n \int_{\mathscr{I}_\alpha}\int_{\partial_T\mathscr{B}_0} [\bar{\boldsymbol{t}}^{*,n}_\alpha(\boldsymbol{X})]_a\, [\delta\dot{\boldsymbol{\varphi}}^n_\alpha(\boldsymbol{X})]^a - h^n \int_{\mathscr{I}_\alpha}\int_{\mathscr{B}_0} [\boldsymbol{P}^{*,n}_\alpha(\boldsymbol{X})]_a{}^A\, [\delta\dot{\boldsymbol{\varphi}}^n_\alpha(\boldsymbol{X})]^a{}_{,A}\end{aligned}} \tag{61}$$

by using the substitution rule and the Frèchet derivative of Eq. (56). Further, the chain rule has been used for the time differentiation of the approximation pertaining to the conjugated momentum field $\boldsymbol{\pi}^n_\alpha$ on $\mathscr{T}_n$. We approximate the time evolution curve $\boldsymbol{\pi}^n$ and the time evolution curve $\delta\dot{\boldsymbol{\varphi}}^n$ corresponding to the time derivative of the variation $\delta\boldsymbol{\varphi}^n$ on $\mathscr{T}^n$, such that

$$\boldsymbol{\pi}^n_\alpha = \sum_{i=1}^{m_{en}} M^i(\alpha)\, \boldsymbol{\pi}^n_{\alpha_i} \qquad \text{and} \qquad \delta\dot{\boldsymbol{\varphi}}^n_\alpha = \sum_{j=1}^{m_{eq}} \tilde{M}^j(\alpha)\, \delta\dot{\boldsymbol{\varphi}}^n_{\tilde{\alpha}_j} \tag{62}$$

respectively. Since the variation $\delta\dot{\boldsymbol{\varphi}}_{\alpha_1}(\boldsymbol{X})$ vanish for all $\boldsymbol{X} \in \mathscr{B}_0$, the deformation $\boldsymbol{\varphi}^n_{\alpha_1}$ coincides with $\boldsymbol{\varphi}_{t^{n-1}_{m_{en}}}$ for all time elements. Now, we transform the integrals in Eq. (43), and subsequently apply the chain rule of differentiation to the approximation of the entropy field η^n_α on $\mathcal{T}^n$. For each $n \in \mathscr{M}_{el}$, we obtain the space-time weak equation

$$\begin{aligned}\int_{\mathscr{I}_\alpha}\int_{\mathscr{B}_0} \partial_\alpha \eta^n_\alpha(\boldsymbol{X})\, \vartheta^n_\alpha(\boldsymbol{X}) &= h_n \int_{\mathscr{I}_\alpha}\int_{\partial_Q\mathscr{B}_0} \frac{\vartheta^n_\alpha(\boldsymbol{X})}{\Theta^n_\alpha(\boldsymbol{X})}\, \overline{Q}^n_\alpha(\boldsymbol{X}) + \\ &+ h_n \int_{\mathscr{I}_\alpha}\int_{\mathscr{B}_0} \frac{\Theta_\infty}{\Theta^n_\alpha(\boldsymbol{X})}\, [\vartheta^n_\alpha(\boldsymbol{X})]_{,A}\, [\boldsymbol{H}^n_\alpha(\boldsymbol{X})]^A + \frac{\vartheta^n_\alpha(\boldsymbol{X})}{\Theta^n_\alpha(\boldsymbol{X})}\, D^{\mathrm{int},n}_\alpha(\boldsymbol{X})\end{aligned} \tag{63}$$

where

$$\eta^n_\alpha = \sum_{i=1}^{m_{en}} M^i(\alpha)\, \eta^n_{\alpha_i} \qquad \text{and} \qquad \Theta^n_\alpha = \sum_{i=1}^{m_{en}} M^i(\alpha)\; \Theta^n_{\alpha_i} \tag{64}$$

The test space for Eq. (63) has to include the time evolution ϑ^n of the relative temperature field. Thus, a variation $\delta\,\Theta^n_{\alpha_1}$ at the lower bound of the continuous curve $\gamma^n_\alpha(s) = \delta\,\Theta^n_s$ only vanish at the boundary $\partial_\Theta\mathscr{B}_0$. We obtain the approximation

$$\delta\,\Theta^n_\alpha = \sum_{i=1}^{m_{en}} M^i(\alpha)\, \delta\,\Theta^n_{\alpha_i} \tag{65}$$

The lower bound $\Theta^n_{\alpha_1}$ of the continuous curve $\gamma^n_\alpha(s) = \Theta^n_s$ thus generally differs from the initial value $\Theta_{t^{n-1}_{m_{en}}}$ of the temperature evolution on each time element. In analogy to Eq. (51), we incorporate the resulting jumps, in an energy-consistent way. For each $\mathcal{T}^n$, $n \in \mathscr{M}_{el}$, the weak form reads

$$\boxed{\begin{aligned}&\int_{\mathscr{B}_0} \frac{[\![\hat{e}^n_{\alpha_1}(\boldsymbol{X})]\!]}{\vartheta^n_{\alpha_1}(\boldsymbol{X})}\, \delta\Theta^n_{\alpha_1}(\boldsymbol{X}) + \int_{\mathscr{I}_\alpha}\int_{\mathscr{B}_0} \partial_\alpha \eta^n_\alpha(\boldsymbol{X})\, \delta\Theta^n_\alpha(\boldsymbol{X}) = h^n \int_{\mathscr{I}_\alpha}\int_{\partial_Q\mathscr{B}_0} \frac{\delta\Theta^n_\alpha(\boldsymbol{X})}{\Theta^n_\alpha(\boldsymbol{X})}\, \overline{Q}^n_\alpha(\boldsymbol{X}) \\ &\qquad + h^n \int_{\mathscr{I}_\alpha}\int_{\mathscr{B}_0} \frac{\Theta_\infty}{\Theta^n_\alpha(\boldsymbol{X})}\, [\delta\Theta^n_\alpha(\boldsymbol{X})]_{,A}\, [\boldsymbol{H}^n_\alpha(\boldsymbol{X})]^A + \delta\Theta^n_\alpha(\boldsymbol{X})\, \frac{D^{\mathrm{int},n}_\alpha(\boldsymbol{X})}{\Theta^n_\alpha(\boldsymbol{X})}\end{aligned}} \tag{66}$$

Finally, we approximate the time evolution of the internal variable field $\boldsymbol{\Gamma}^n_\alpha$, pointwise determined on $\mathcal{T}^n$, due to the isoparametric concept. According to Eq. (53), the test space has to include the time evolution $\dot{\boldsymbol{\Gamma}}^n$ pertaining to the time derivative of the internal variable field on $\mathscr{T}_n$. We therefore arrive at the approximations

$$\boldsymbol{\Gamma}^n_\alpha = \sum_{i=1}^{m_{en}} M^i(\alpha)\, \boldsymbol{\Gamma}^n_{\alpha_i} \qquad \text{and} \qquad \delta\dot{\boldsymbol{\Gamma}}^n_\alpha = \sum_{j=1}^{m_{eq}} \tilde{M}^j(\alpha)\, \delta\dot{\boldsymbol{\Gamma}}^n_{\tilde{\alpha}_j} \tag{67}$$

for Eq. (53) on the parent domain. Thereby, the conditions $[\delta\dot{\boldsymbol{\Gamma}}_{\alpha_1}(\boldsymbol{X})]_{AB} = 0$ are fulfilled for all $\boldsymbol{X} \in \mathscr{B}_0$. We divide each integral of Eq. (53) into m_{el} sub-integrals. In the light of the constant Frèchet derivative of Eq. (56), we apply the substitution rule to the time integrals and the chain rule of differentiation to the time derivative. For each $n \in \mathscr{M}_{el}$, we so get at

$$\boxed{\begin{aligned} &h_n \int_{\mathscr{I}_\alpha} [\,\boldsymbol{\Upsilon}^n_\alpha(\boldsymbol{X})]^{AF}\, [\delta\dot{\boldsymbol{\Gamma}}^n_\alpha(\boldsymbol{X})]_{AF} = \\ &\quad \frac{1}{4}\int_{\mathscr{T}} [\delta\dot{\boldsymbol{\Gamma}}^n_\alpha(\boldsymbol{X})]_{AF} [\{\boldsymbol{\Gamma}^n_\alpha(\boldsymbol{X})\}^{-1}]^{FB}\; V^A{}_B{}^C{}_D\; [\partial_\alpha \boldsymbol{\Gamma}^n_\alpha(\boldsymbol{X})]_{CE}\, [\{\boldsymbol{\Gamma}^n_\alpha(\boldsymbol{X})\}^{-1}]^{ED} \end{aligned}} \tag{68}$$

for any $\boldsymbol{X} \in \mathscr{B}_0$. We approximate the tensor $\boldsymbol{\Upsilon}^n_\alpha(\boldsymbol{X})$ such that it lies for any time $\alpha \in \mathscr{I}_\alpha$ in the cotangent space at the internal variable evolution. In order to obtain in a weak form a unique interpolation of the temporal test function at each temporal quadrature point, a family of m shape functions has to be evaluated at exactly m distinct quadrature points. Since we approximate the test function associated with Eq. (66) with one Lagrange polynomial more as compared to the other weak forms, we have to use one quadrature point more. Therefore, in the following, we endue the symbol $\mathscr{I}_\alpha$ of the time integration domain associated with Eq. (66) with the suffix η to refer to this different number of quadrature points.

4.2 The spatial finite element approximation

We consider a partition of $\mathscr{B}_0$ into $n_{el} \geqslant 1$ disjoint sub-domains $\mathscr{B}^e_0$, $e \in \mathscr{N}_{el} = \{1, \ldots, n_{el}\}$, called the e-th element of $\mathscr{B}_0$. The union of all these spatial elements, in turn, is given by $\mathscr{B}_0$. Each element $\mathscr{B}^e_0$ is defined by points ${}^e\boldsymbol{X}^a$, $a \in \mathscr{N}_{en} = \{1, \ldots, n_{en}\}$, called the spatial nodes. We define index sets $\mathscr{N}^e_\varphi = \{a \in \mathscr{N}_{en} | {}^e\boldsymbol{X}^a \in \partial_\varphi \mathscr{B}_0\}$ to indicate which element nodes lie on the mechanical Dirichlet boundary. We introduce a spatial parent domain $\mathscr{B}_\Box$, which is mapped on a spatial element $\mathscr{B}^e_0$ by

$$\boldsymbol{\psi}^e_0 : \mathscr{B}_\Box \ni \boldsymbol{\eta} \mapsto \sum_{a \in \mathscr{N}_{en}} N_a(\boldsymbol{\eta})\, {}^e\boldsymbol{X}^a \in \mathscr{B}^e_0 \tag{69}$$

The properties $N_a(\boldsymbol{\eta}^b) = \delta^b{}_a$, $a, b \in \mathscr{N}_{en}$, of the Lagrange polynomials $N_a : \mathscr{B}_\Box \to \mathbb{R}$ provides that the nodes $\boldsymbol{\eta}^b \in \mathscr{B}_\Box$ are mapped to the spatial nodes ${}^e\boldsymbol{X}^b = \boldsymbol{\psi}^e(\boldsymbol{\eta}^b)$. Consider a curve $C^e(s) = {}^e\boldsymbol{X}_s$ in $\mathscr{B}^e_0$, and a curve $\boldsymbol{\gamma}_\Box(s) = \boldsymbol{\eta}_s$ in $\mathscr{B}_\Box$. Differentiation of Eq. (69) implies a linear relation between the tangent vectors at ${}^e\boldsymbol{X} \in \mathscr{B}^e_0$ and $\boldsymbol{\eta} \in \mathscr{B}_\Box$, respectively, which reads

$$T_X \mathscr{B}^e_0 \ni {}^e\boldsymbol{W} = \mathrm{D}\boldsymbol{\psi}^e_0(\boldsymbol{\eta})\, \boldsymbol{\nu}_\eta \in T_\eta \mathscr{B}_\Box \tag{70}$$

The volume element V^e_X at ${}^e\boldsymbol{X} \in \mathscr{B}^e_0$ is mapped by the Jacobian determinant of Eq. (69), given by $J^e(\boldsymbol{\eta}) = \det(\mathrm{D}\boldsymbol{\psi}^e_0(\boldsymbol{\eta}))$, to the volume element V_η at $\boldsymbol{\eta} \in \mathscr{B}_\Box$. The partition of $\mathscr{B}_0$ divides volume integrals into a sum of n_{el} sub-integrals with respect to the spatial elements $\mathscr{B}^e_0$, $e \in \mathscr{N}_{el}$.

Transforming each material point ${}^e\boldsymbol{X} \in \mathscr{B}_0^e$ to the spatial parent domain, Eq. (59) takes the form

$$\boxed{\int_{\mathscr{I}_\alpha}\int_{\mathscr{B}_\square} [\delta\dot{\boldsymbol{\pi}}_\alpha^{n,e}(\boldsymbol{\eta})]_a \, [\partial_\alpha \boldsymbol{\varphi}_\alpha^{n,e}(\boldsymbol{\eta})]^a J^e(\boldsymbol{\eta}) = h^n \int_{\mathscr{I}_\alpha}\int_{\mathscr{B}_\square} [\delta\dot{\boldsymbol{\pi}}_\alpha^{n,e}(\boldsymbol{\eta})]_a \, [\boldsymbol{v}_\alpha^{n,e}(\boldsymbol{\eta})]^a J^e(\boldsymbol{\eta})} \tag{71}$$

for all $(n,e) \in \mathscr{M}_{el} \times \mathscr{N}_{el}$, where the notation $\boldsymbol{\varphi}_\alpha^{n,e}(\boldsymbol{\eta}) = [\boldsymbol{\varphi}_\alpha^n|_{\mathscr{B}_0^e} \circ \boldsymbol{\psi}_0^e](\boldsymbol{\eta})$ has been introduced. In the isoparametric concept, the deformation $\boldsymbol{\varphi}_\alpha^{n,e}$ of the spatial element $\mathscr{B}_0^e$ during the time element $\mathscr{T}^n$ is approximated in space analogously to Eq. (69). After using Eq. (58), there remains to approximate the deformations $\boldsymbol{\varphi}_{\alpha_i}^{n,e}$ at the nodes $\alpha_i \in \mathscr{I}_\alpha$. We assume

$$\boldsymbol{\varphi}_{\alpha_i}^{n,e}(\boldsymbol{\eta}) = \sum_{a \in \mathscr{N}_{en} \setminus \mathscr{N}_\varphi^e} N_a(\boldsymbol{\eta}) \, {}^e\boldsymbol{x}_{\alpha_i}^a + \sum_{a \in \mathscr{N}_\varphi^e} N_a(\boldsymbol{\eta}) \, {}^e\boldsymbol{X}^a \tag{72}$$

The last sum arise from Eq. (17). The velocity $\boldsymbol{v}_\alpha^{n,e}$ is an element of the tangent space of the motion, and the test function $\delta\dot{\boldsymbol{\pi}}_\alpha^{n,e}$ lies in the corresponding cotangent space. With exception of the different boundary conditions, these tangent and cotangent vectors are approximated as the corresponding deformation. Hence, we obtain

$$\boldsymbol{v}_{\alpha_i}^{n,e}(\boldsymbol{\eta}) = \sum_{a \in \mathscr{N}_{en} \setminus \mathscr{N}_\varphi^e} N_a(\boldsymbol{\eta}) \, {}^e\boldsymbol{v}_{\alpha_i}^a \qquad \text{and} \qquad \delta\dot{\boldsymbol{\pi}}_{\tilde{\alpha}_j}^{n,e}(\boldsymbol{\eta}) = \sum_{a \in \mathscr{N}_{en} \setminus \mathscr{N}_\varphi^e} N_a(\boldsymbol{\eta}) \, {}^e\delta\boldsymbol{\pi}_{\tilde{\alpha}_j}^a \tag{73}$$

according to the vanishing Dirichlet boundary conditions in the corresponding spaces. To account for the Neumann boundary $\partial_T\mathscr{B}_0$, we define the set $\mathscr{N}_T^e = \{a \in \mathscr{N}_{en} | {}^e\boldsymbol{X}^a \in \partial_T\mathscr{B}_0\}$, indicating nodes of the element $\mathscr{B}_0^e$, which lie on its Neumann boundary $\partial_T\mathscr{B}_0^e$. Then, we introduce a transformation

$$\bar{\psi}_0^e : \partial\mathscr{B}_\square \ni \bar{\eta} \mapsto \sum_{a \in \mathscr{N}_T^e} \bar{N}_a(\bar{\eta}) \, {}^e\boldsymbol{X}^a \in \partial\mathscr{B}_0^e \tag{74}$$

from a parent domain $\partial\mathscr{B}_\square$ to the e-th (Neumann) boundary element $\partial\mathscr{B}_0^e$. The shape functions $\bar{N}_a : \partial\mathscr{B}_\square \to \mathbb{R}$ are also Lagrange polynomials satisfying the condition $\bar{N}_a(\bar{\eta}^b) = \delta^b{}_a$. Therefore, nodes $\bar{\eta}^b \in \partial\mathscr{B}_\square$ are mapped to nodes ${}^e\boldsymbol{X}^b = \bar{\psi}^e(\bar{\eta}^b) \in \partial\mathscr{B}_0^e$. After dividing up the spatial integrals in Eq. (61), the Eqs. (69) and (74) provides the weak form

$$\boxed{\begin{gathered}\int_{\mathscr{I}_\alpha}\int_{\mathscr{B}_\square} [\partial_\alpha \boldsymbol{\pi}_\alpha^{n,e}(\boldsymbol{\eta})]_a \, [\delta\dot{\boldsymbol{\varphi}}_{\tilde{\alpha}}^{n,e}(\boldsymbol{\eta})]^a J^e(\boldsymbol{\eta}) = h^n \int_{\mathscr{I}_\alpha}\int_{\partial\mathscr{B}_\square} [\bar{\boldsymbol{t}}_\alpha^{*,n,e}(\bar{\eta})]_a \, [\delta\dot{\boldsymbol{\varphi}}_{\tilde{\alpha}}^{n,e}(\bar{\eta})]^a \bar{J}^e(\bar{\eta}) - \\ -h^n \int_{\mathscr{I}_\alpha}\int_{\mathscr{B}_\square} [\boldsymbol{P}_\alpha^{*,n,e}(\boldsymbol{\eta})]_a{}^A \, [\delta\dot{\boldsymbol{\varphi}}_{\tilde{\alpha}}^{n,e}(\boldsymbol{\eta})]^a{}_{,A} J^e(\boldsymbol{\eta})\end{gathered}} \tag{75}$$

for all $(n,e) \in \mathscr{M}_{el} \times \mathscr{N}_{el}$. The mapping $\bar{J}^e(\bar{\eta}) = \det(\mathrm{D}\bar{\psi}_0^e(\bar{\eta}))$ denotes the Jacobian determinant of Eq. (74). The Lagrangian momentum fields $\boldsymbol{\pi}_{\alpha_i}^{n,e}$ at the nodes $\alpha_i \in \mathscr{I}_\alpha$ lie in the cotangent space of the motion, whereas the test functions $\delta\dot{\boldsymbol{\varphi}}_{\tilde{\alpha}_j}^{n,e}$ are elements of the corresponding tangent space. Hence, we apply Eq. (73) to these fields. The spatial distribution of the first Piola-Kirchhoff traction vector field $\bar{\boldsymbol{t}}_\alpha^{n,e}$ at time $\alpha \in \mathscr{I}_\alpha$ is approximated by

$$\bar{\boldsymbol{t}}_\alpha^{n,e}(\bar{\eta}) = \sum_{a \in \mathscr{N}_T^e} \bar{N}_a(\bar{\eta}) {}^e\boldsymbol{t}_\alpha^a \tag{76}$$

The vectors ${}^e\boldsymbol{t}_\alpha^a$ denote given traction loads on the boundary notes. In the last term on the righthand side of Eq. (75), we have to determine the gradient with respect to a point ${}^e\boldsymbol{X} \in \mathscr{B}_0^e$.

For this purpose, we multiply Eq. (70) with the inverse Jacobian $(\mathrm{D}\boldsymbol{\psi}_0^e)^{-1}$ pertaining to Eq. (69). We obtain so the relation between tangent vectors at a curve $\boldsymbol{\gamma}_{\square}(s) = \boldsymbol{\eta}_s$ in $\mathscr{B}_{\square}$ and at a curve $C^e(s) = {}^e\boldsymbol{X}_s$ in $\mathscr{B}_0^e$. The gradient of the test function then reads

$$[\delta\dot{\boldsymbol{\varphi}}_\alpha^{n,e}]^a{}_{,A} = [\delta\dot{\boldsymbol{\varphi}}_\alpha^{n,e}]^a{}_{,i}\,[(\mathrm{D}\boldsymbol{\psi}_0^e)^{-1}]^i{}_A \tag{77}$$

where i indicates the coordinates in $\mathscr{B}_{\square}$. To incorporate the thermal boundary conditions, we define index sets $\mathscr{N}_\Theta^e = \{a \in \mathscr{N}_{en} | {}^e\Theta^a \in \partial_\Theta\mathscr{B}_0\}$ to indicate nodes on the thermal Dirichlet boundary $\partial_\Theta\mathscr{B}_0$, and index sets $\mathscr{N}_Q^e = \{a \in \mathscr{N}_{en} | {}^e\Theta^a \in \partial_Q\mathscr{B}_0\}$ to designate nodes on the thermal Neumann boundary $\partial_Q\mathscr{B}_0$. Considering the partition of $\mathscr{B}_0$, and relating spatial integrals to the corresponding parent domains, Eq. (66) reads

$$\boxed{\begin{aligned}&\int_{\mathscr{B}_\square} \frac{[\![\hat{e}_{\alpha_1}^{n,e}(\boldsymbol{\eta})]\!]}{\vartheta_{\alpha_1}^{n,e}(\boldsymbol{\eta})}\;\delta\Theta_{\alpha_1}^{n,e}(\boldsymbol{\eta})\,J^e(\boldsymbol{\eta}) + \int_{\mathscr{I}_\alpha^\eta}\int_{\mathscr{B}_\square} \partial_\alpha \eta_\alpha^{n,e}(\boldsymbol{\eta})\,\delta\Theta_\alpha^{n,e}(\boldsymbol{\eta})\,J^e(\boldsymbol{\eta}) = \\ &\quad h^n \int_{\mathscr{I}_\alpha^\eta}\int_{\mathscr{B}_\square}\left\{\frac{\Theta_\infty}{\Theta_\alpha^{n,e}(\boldsymbol{\eta})}\,[\delta\Theta_\alpha^{n,e}(\boldsymbol{\eta})]_{,A}\,[\boldsymbol{H}_\alpha^{n,e}(\boldsymbol{\eta})]^A + \delta\Theta_\alpha^{n,e}(\boldsymbol{\eta})\,\frac{D_\alpha^{\mathrm{int},n,e}(\boldsymbol{\eta})}{\Theta_\alpha^{n,e}(\boldsymbol{\eta})}\right\} J^e(\boldsymbol{\eta}) + \\ &\quad + h^n \int_{\mathscr{I}_\alpha^\eta}\int_{\partial\mathscr{B}_\square} \frac{\delta\Theta_\alpha^{n,e}(\bar{\eta})}{\Theta_\alpha^{n,e}(\bar{\eta})}\,\overline{Q}_\alpha^{n,e}(\bar{\eta})\,\bar{J}^e(\bar{\eta})\end{aligned}} \tag{78}$$

for all $(n, e) \in \mathscr{M}_{el} \times \mathscr{N}_{el}$. The geometric approximation of the thermal Neumann boundary coincides with that of the mechanical Neumann boundary. By following the isoparametric concept, we approximate the Lagrangian temperature field $\Theta_\alpha^{n,e}$ on the element $\mathscr{B}_0^e$ during the time interval $\mathscr{T}^n$ analogously to the deformation. We obtain the approximation

$$\Theta_{\alpha_i}^{n,e}(\boldsymbol{\eta}) = \sum_{a\in\mathscr{N}_{en}\setminus\mathscr{N}_\Theta^e} N_a(\boldsymbol{\eta})\,{}^e\Theta_{\alpha_i}^a + \sum_{a\in\mathscr{N}_\Theta^e} N_a(\boldsymbol{\eta})\;\Theta_\infty \tag{79}$$

by taking into account the constant environment temperature Θ_∞ on the thermal Dirichlet boundary. Likewise, we approximate the test function $\delta\Theta_{\alpha_i}^{n,e}$ at the nodes in the parent domain in conjunction with Eq. (73). The entropy field $\eta_{\alpha_i}^{n,e}$ is approximated such that it lies in the cotangent space at the temperature evolution. We define

$$\eta_{\alpha_i}^{n,e}(\boldsymbol{\eta}) = -\frac{\partial\Psi(\boldsymbol{\Gamma}_{\alpha_i}^{n,e}(\boldsymbol{\eta}), \boldsymbol{C}_{\alpha_i}^{n,e}(\boldsymbol{\eta}), \Theta_{\alpha_i}^{n,e}(\boldsymbol{\eta}))}{\partial\Theta} \qquad \text{and} \qquad \delta\Theta_{\alpha_i}^{n,e}(\boldsymbol{\eta}) = \sum_{a\in\mathscr{N}_{en}\setminus\mathscr{N}_\Theta^e} N_a(\boldsymbol{\eta})\,{}^e\delta\Theta_{\alpha_i}^a \tag{80}$$

Since we determine the Lagrangian internal variable field $\boldsymbol{\Gamma}_\alpha^{n,e}(\boldsymbol{\eta})$ at the considered points $\boldsymbol{\eta} \in \mathscr{B}_{\square}$ in the spatial parent domain, we desist from a spatial approximation. The approximation $\boldsymbol{C}_{\alpha_i}^{n,e}(\boldsymbol{\eta})$ of the right Cauchy-Green tensor pertaining to the e-th spatial element during the n-th time element follows from Eq. (1), via the approximation $\boldsymbol{F}_{\alpha_i}^{n,e}(\boldsymbol{\eta})$ of the corresponding deformation gradient, given by

$$[\boldsymbol{F}_{\alpha_i}^{n,e}(\boldsymbol{\eta})]^a{}_A = [\nabla\boldsymbol{\varphi}_{\alpha_i}^{n,e}(\boldsymbol{\eta})]^a{}_j\,[(\mathrm{D}\boldsymbol{\psi}_0^e)^{-1}(\boldsymbol{\eta})]^j{}_A \tag{81}$$

Assume that the normal inward heat flux $\overline{Q}_\alpha^{n,e}$ on the thermal Neumann boundary $\partial_Q\mathscr{B}_0^e$ is also given in dependence of the time $\alpha \in \mathscr{I}_\alpha$. We define inward normal projections ${}^e\overline{Q}_\alpha^a$ of the heat flux at the nodes of the boundary element, which are distributed by

$$\overline{Q}_\alpha^{n,e}(\bar{\eta}) = \sum_{a\in\mathscr{N}_Q^e} \bar{N}_a(\bar{\eta})\,{}^e\overline{Q}_\alpha^a \tag{82}$$

along the corresponding element boundary.

5 THE TIME APPROXIMATION OF THE CONSTITUTIVE FIELDS

In order to maintain the conservation laws and the stability estimate in the discrete setting, we have to supplement the weak forms. First, we consider the directional derivative along the continuous time curve $\boldsymbol{\gamma}_t^n(s) = \mathcal{L}(t+s)$ in the n-th time element. We integrate this derivative in time, and obtain

$$\int_{\mathscr{T}^n} \dot{\mathcal{L}}(t) = \sum_{e=1}^{n_{el}} \int_{\mathscr{I}_\alpha} \int_{\mathscr{B}_\square} [\partial_\alpha \boldsymbol{\pi}_\alpha^{n,e}(\boldsymbol{\eta})]_a \, [\boldsymbol{\xi}_0]^a J^e(\boldsymbol{\eta}) \tag{83}$$

If we employ Eq. (62), the time integration concerns only the temporal shape functions. Since this time integrals can be computed exactly, the fundamental theorem of calculus is fulfilled. Nevertheless, the vector $\boldsymbol{\xi}_0 \in \mathscr{A}$ is constant, it is an admissible test function $\delta\dot{\boldsymbol{\varphi}}_\alpha^{n,e}(\boldsymbol{\eta})$ of Eq. (75), due to the completeness condition of the Lagrange polynomials. We employ this test function in Eq. (75), and obtain the identity

$$\int_{\mathscr{I}_\alpha} \int_{\mathscr{B}_\square} [\partial_\alpha \boldsymbol{\pi}_\alpha^{n,e}(\boldsymbol{\eta})]_a \, [\boldsymbol{\xi}_0]^a J^e(\boldsymbol{\eta}) = -h^n \int_{\mathscr{I}_\alpha} \int_{\mathscr{B}_\square} [\boldsymbol{P}_\alpha^{*,n,e}(\boldsymbol{\eta})]_a{}^A \, [\boldsymbol{\xi}_0]^a{}_{,A} J^e(\boldsymbol{\eta}) = 0 \tag{84}$$

Since Eq. (84) coincides with the difference $\mathcal{L}(t^{n+1}) - \mathcal{L}(t^n)$, we obtain total linear momentum conservation for an arbitrary approximation of the covariant first Piola-Kirchhoff stress tensor, and for an arbitrary time step size. On the other hand, the directional derivative along the continuous time curve $\boldsymbol{\gamma}_t^n(s) = \mathcal{J}(t+s)$ in the n-th time element in conjunction with time integration leads to

$$\sum_{e=1}^{n_{el}} \int_{\mathscr{I}_\alpha} \int_{\mathscr{B}_\square} \epsilon_{abc} \delta^{cd} [\boldsymbol{\xi}_0]^a \left\{ [\partial_\alpha \boldsymbol{\varphi}_\alpha^{n,e}(\boldsymbol{\eta})]^b [\boldsymbol{\pi}_\alpha^{n,e}(\boldsymbol{\eta})]_d + [\boldsymbol{\varphi}_\alpha^{n,e}(\boldsymbol{\eta})]^b [\partial_\alpha \boldsymbol{\pi}_\alpha^{n,e}(\boldsymbol{\eta})]_d \right\} J^e(\boldsymbol{\eta}) \tag{85}$$

If we employ the Eqs. (58) and (62), the fundamental theorem of calculus with respect to $\mathcal{J}(t)$ is fulfilled, because the time integrals can be calculated exactly. Eq. (85) therefore coincides with $\mathcal{J}(t^{n+1}) - \mathcal{J}(t^n)$. Now, we have to employ Eq. (71) in the first term, however, in Eq. (85), the corresponding test function is not interpolated by the Lagrange polynomials $\{\tilde{M}^j(\alpha)\}_{j=1}^{m_{eq}}$ at the temporal test nodes $\tilde{\alpha}_j$, $j = 1, \ldots, m_{eq}$. Therefore, we determine nodal values $\boldsymbol{\pi}_{\tilde{\alpha}_j}^{n,e}(\boldsymbol{\eta})$ by solving uniquely the linear system of equations

$$\sum_{j=1}^{m_{eq}} \tilde{M}^j(\tilde{\xi}_k) \boldsymbol{\pi}_{\tilde{\alpha}_j}^{n,e}(\boldsymbol{\eta}) = \sum_{i=1}^{m_{en}} M^i(\tilde{\xi}_k) \boldsymbol{\pi}_{\alpha_i}^{n,e}(\boldsymbol{\eta}) \tag{86}$$

at m_{eq} quadrature points ξ_k, $k = 1, \ldots, m_{eq}$. Thereupon, the first term of Eq. (85) vanish independent of the time step size, according to the skew-symmetry of the permutation symbol. In the second term of Eq. (85), we employ Eq. (75). For this purpose, we determine nodal values $\boldsymbol{\varphi}_{\tilde{\alpha}_j}^{n,e}(\boldsymbol{\eta})$ by a corresponding linear system of the form, given in Eq. (86). Taking the definitions of the deformation gradient and of the Kirchhoff stress tensor into account, the second term of Eq. (85) is given by

$$-h^n \int_{\mathscr{I}_\alpha} \int_{\mathscr{B}_\square} \epsilon_{acb} [\boldsymbol{\xi}_0]^a [\boldsymbol{\tau}_\alpha^{n,e}(\boldsymbol{\eta})]^{cb} J^e(\boldsymbol{\eta}) \tag{87}$$

Postulating the symmetry of the Kirchhoff stress tensor approximation, this term vanishes due to the skew-symmetry of the permutation symbol. Since both terms of Eq. (85) vanish, we obtain total angular momentum conservation for any time step size. Now, we consider the directional derivative along the continuous time curve $\boldsymbol{\gamma}_t^n(s) = \mathcal{T}(t+s)$ in the n-th time element. Time integration leads to

$$\int_{\mathscr{T}^n} \dot{\mathcal{T}}(t) = \sum_{e=1}^{n_{el}} \int_{\mathscr{I}_\alpha} \int_{\mathscr{B}_\square} [\partial_\alpha \boldsymbol{\pi}_\alpha^{n,e}(\boldsymbol{\eta})]_a \, [\boldsymbol{v}_\alpha^{n,e}(\boldsymbol{\eta})]^a J^e(\boldsymbol{\eta}) \tag{88}$$

If we employ the Eqs. (58) and (62), the time integration concerns only the temporal shape functions. The fundamental theorem of calculus is therefore exactly fulfilled, and the righthand side coincides with the difference $\mathcal{T}(t^{n+1}) - \mathcal{T}(t^n)$. Since the derivative $\partial_\alpha \boldsymbol{\pi}_\alpha^{n,e}(\boldsymbol{\eta})$ is an admissible test function for Eq. (71), we employ this equation as next step. Moreover, the derivative $\partial_\alpha \boldsymbol{\varphi}_\alpha^{n,e}(\boldsymbol{\eta})$ of the deformation approximation lies in the test space of Eq. (75). Therefore, we subsequently employ Eq. (75). We arrive at the kinetic energy balance

$$\mathcal{T}(t^{n+1}) - \mathcal{T}(t^n) = -\sum_{e=1}^{n_{el}} \int_{\mathscr{I}_\alpha} \int_{\mathscr{B}_\square} [\boldsymbol{P}_\alpha^{*,n,e}(\boldsymbol{\eta})]_a{}^A \, [\partial_\alpha \boldsymbol{\varphi}_\alpha^{n,e}(\boldsymbol{\eta})]^a{}_{,A} J^e(\boldsymbol{\eta}) \tag{89}$$

Now, we determine the directional derivative along the continuous time curve $\boldsymbol{\gamma}_t^n(s) = \mathcal{E}(t+s)$ in the n-th time element. At the time integration of this derivative, we bear in mind the different quadrature rules in the discrete setting. Noticing the definition of the relative internal energy density as well as the cotangent vectors pertaining to the free energy, we obtain the relation

$$\begin{aligned} \int_{\mathscr{I}_\alpha} \int_{\mathscr{B}_\square} \partial_\alpha \hat{e}_\alpha^{n,e}(\boldsymbol{\eta}) = & \int_{\mathscr{I}_\alpha^\eta} \int_{\mathscr{B}_\square} \partial_\alpha \eta_\alpha^{n,e}(\boldsymbol{\eta}) \, \vartheta_\alpha^{n,e}(\boldsymbol{\eta}) \, J^e(\boldsymbol{\eta}) + \\ & + \int_{\mathscr{I}_\alpha} \int_{\mathscr{B}_\square} \left\{ [\boldsymbol{P}_\alpha^{*,n,e}(\boldsymbol{\eta})]_a{}^A \, [\partial_\alpha \boldsymbol{F}_\alpha^{n,e}(\boldsymbol{\eta})]^a{}_A - [\boldsymbol{\Upsilon}_\alpha^{n,e}(\boldsymbol{\eta})]^{AB} \, [\partial_\alpha \boldsymbol{\Gamma}_\alpha^{n,e}(\boldsymbol{\eta})]_{AB} \right\} J^e(\boldsymbol{\eta}) \end{aligned} \tag{90}$$

for all $(n,e) \in \mathscr{M}_{el} \times \mathscr{N}_{el}$. Recall the mapping $\boldsymbol{C}_\alpha^n = [\boldsymbol{C}|_{\mathscr{T}^n} \circ \tau^n](\alpha)$ designates the right Cauchy-Green tensor field during the n-th time element at any time point $\alpha \in \mathscr{I}_\alpha$ in the temporal parent domain. We approximate the time evolution of the corresponding right Cauchy-Green tensor $\boldsymbol{C}_\alpha^{n,e}(\boldsymbol{\eta})$ pertaining to the e-th spatial element, such that

$$\boldsymbol{C}_\alpha^{n,e}(\boldsymbol{\eta}) = \sum_{i=1}^{m_{en}} M^i(\alpha) \, \boldsymbol{C}_{\alpha_i}^{n,e}(\boldsymbol{\eta}) \tag{91}$$

Note that the approximated stress power $\mathcal{P}^{\text{int},n,e}(\alpha)$ based on the second Piola-Kirchhoff stress tensor in conjunction with Eq. (91) does not coincide with the stress power in Eq. (75). Furthermore, the time integration in Eq. (90) is, in general, not computable exactly. Hence, we have to enforce the fundamental theorem of calculus with respect to $\hat{e}_\alpha(\boldsymbol{\eta})$. Noticing the derivation of the jump term by formulating a minimisation problem, we state a corresponding constraint $\mathcal{G}_S(\hat{\boldsymbol{S}}_\alpha^{n,e}(\boldsymbol{\eta}))$ by taking Eq. (4) into account. Since we need a symmetric approximation of the Kirchhoff stress tensor, we determine a trace tensor corresponding to the second Piola-Kirchhoff stress. We obtain an isoperimetrical problem associated with an augmented Lagrange functional, and arrive at the integral term

$$-h^n \int_{\mathscr{B}_\square} \frac{\hat{e}_{\alpha_{m_{en}}}^{n,e}(\boldsymbol{\eta}) - \hat{e}_{\alpha_1}^{n,e}(\boldsymbol{\eta}) - \displaystyle\int_{\mathscr{I}_\alpha} \partial_\alpha \hat{e}_\alpha^{n,e}(\boldsymbol{\eta})}{\displaystyle\int_{\mathscr{I}_\alpha} [\hat{\boldsymbol{P}}_\alpha^{*,n,e}(\boldsymbol{\eta})]_a{}^A \, [\partial_\alpha \boldsymbol{\varphi}_\alpha^{n,e}(\boldsymbol{\eta})]^a{}_{,A}} \int_{\mathscr{I}_\alpha} [\hat{\boldsymbol{P}}_\alpha^{*,n,e}(\boldsymbol{\eta})]_a{}^A \, [\delta \dot{\boldsymbol{\varphi}}_{\tilde{\alpha}}^{n,e}(\boldsymbol{\eta})]^a{}_{,A} J^e(\boldsymbol{\eta}) \tag{92}$$

which we add on the righthand side of Eq. (75). The components $[\hat{\boldsymbol{P}}_\alpha^{*,n,e}(\boldsymbol{\eta})]_a{}^A$ coincide with the sums $\delta_{ab}[\boldsymbol{F}_\alpha^{n,e}(\boldsymbol{\eta})]^b{}_B\,[\partial_\alpha \boldsymbol{C}_\alpha^{*,n,e}(\boldsymbol{\eta})]^{BA}$. This additional term of Eq. (75) annihilate the stress power in Eq. (89) completely, and introduce the relative internal energy density behind the jump. Recall, we arrived at the stability estimate by the assumption that the time integrals of the internal dissipation, calculated in the Eqs. (51) and (54), are identical. In the discrete setting, however, we have to enforce this property. Consequently, we formulate a corresponding constraint for a viscosity trace tensor in the internal dissipation. Let $\boldsymbol{D}_\alpha^{n,e}(\boldsymbol{\eta})$ denote the approximated viscous strain rate tensor on the e-th spatial element at any time point $\alpha \in \mathscr{I}_\alpha$, defined by the components $[\partial_\alpha \boldsymbol{\Gamma}_\alpha^{n,e}(\boldsymbol{\eta})]_{AB}[(\boldsymbol{\Gamma}_\alpha^{n,e}(\boldsymbol{\eta}))^{-1}]^{BC}/(2h^n)$. After employing the obtained viscosity trace tensor in Eq. (16), we arrive at the integral term

$$h^n \int_{\mathscr{B}_\square} \frac{\displaystyle\int_{\mathscr{I}_\alpha} D_\alpha^{\mathrm{int},n,e}(\boldsymbol{\eta}) - \int_{\mathscr{I}_\alpha^\eta} D_\alpha^{\mathrm{int},n,e}(\boldsymbol{\eta})}{\displaystyle\int_{\mathscr{I}_\alpha^\eta} \left\{ \frac{\vartheta_\alpha^{n,e}(\boldsymbol{\eta})}{\Theta_\alpha^{n,e}(\boldsymbol{\eta})} \hat{D}_\alpha^{\mathrm{int},n,e}(\boldsymbol{\eta}) \right\}^2} \int_{\mathscr{I}_\alpha^\eta} \delta\,\Theta_\alpha^{n,e}(\boldsymbol{\eta}) \frac{\vartheta_\alpha^{n,e}(\boldsymbol{\eta})}{\{\Theta_\alpha^{n,e}(\boldsymbol{\eta})\}^2} \left\{ \hat{D}_\alpha^{\mathrm{int},n,e}(\boldsymbol{\eta}) \right\}^2 J^e(\boldsymbol{\eta}) \tag{93}$$

which we add on the righthand side of Eq. (78). The function $\hat{D}_\alpha^{\mathrm{int},n,e}(\boldsymbol{\eta})$ denotes the sum $[\boldsymbol{D}_\alpha^{*,n,e}(\boldsymbol{\eta})]^A{}_B[\boldsymbol{D}_\alpha^{n,e}(\boldsymbol{\eta})]_A{}^B$ associated with the viscous strain rate tensor. Due to the spatial finite element approximation, we solve Eq. (68) at the considered points $\boldsymbol{\eta} \in \mathscr{B}_\square$ in the spatial parent domain. Employing the time derivative $\partial_\alpha \boldsymbol{\Gamma}_\alpha^n(\boldsymbol{\eta})$ as admissible test function, the righthand side of Eq. (68) coincides with the internal dissipation $D_\alpha^{\mathrm{int},n,e}(\boldsymbol{\eta})$ in the e-th spatial element. Therefore, we arrive at the stability estimate

$$\boxed{\mathcal{V}(t^{n+1}) - \mathcal{V}(t^n) = -h^n \sum_{e=1}^{n_{el}} \int_{\mathscr{I}_\alpha^\eta} \int_{\mathscr{B}_\square} \frac{\Theta_\infty}{\Theta_\alpha^{n,e}(\boldsymbol{\eta})}\, D_\alpha^{\mathrm{tot},n,e}(\boldsymbol{\eta})\, J^e(\boldsymbol{\eta}) \leqslant 0} \tag{94}$$

which coincides with Eq. (34). In the discrete setting, we apply the Gaussian quadrature rule. Hence, the existing time integrals associated with the temporal shape functions are calculated exactly, which is important for the conservation laws and the kinetic energy balance as verified.

6 NUMERICAL EXAMPLE

The simulation snapshot shows a free unloaded motion of a tyre with a small uninsulated portion ($h^n = 0.1$). The motion is initiated through initial velocities. The stiff material with a strong thermo-mechanical coupling is described by a thermo-dynamically extended neo-Hookean material model, together with a constant conductivity and viscosity. The colours indicate the absolute body temperature. The free unloaded motion cause conserved momentum maps (see Fig. 1). As expected for the ehG method, the absolute residual value of Eq. (94) is less than the tolerance $\epsilon = 10^{-8}$ pertaining to the Newton-Raphson method. Hence, the Lyapunov function is steady decreasing till the equilibrium state is reached. For comparison, we implemented the hG method without the correcting terms, given by Eq. (92) and Eq. (93), and with the standard approximation

$$[\boldsymbol{C}_\alpha^{n,e}(\boldsymbol{\eta})]_{AB} = [(\boldsymbol{F}_\alpha^{n,e}(\boldsymbol{\eta}))^T]_A{}^a \delta_{ab}\,[\boldsymbol{F}_\alpha^{n,e}(\boldsymbol{\eta})]^b{}_B \tag{95}$$

of the right Cauchy-Green tensor, arising from an approximation of the time evolution *after* a spatial approximation of the corresponding field. In Ref. [1], we show that Eq. (95) leads to approximation errors, having a physical effect. The hG method do not fulfil the stability estimate in the discrete setting (see Fig. 1), and therefore diverge after a few calculated time steps of the length $h^n = 0.1$. Both momentum maps are conserved till the divergence.

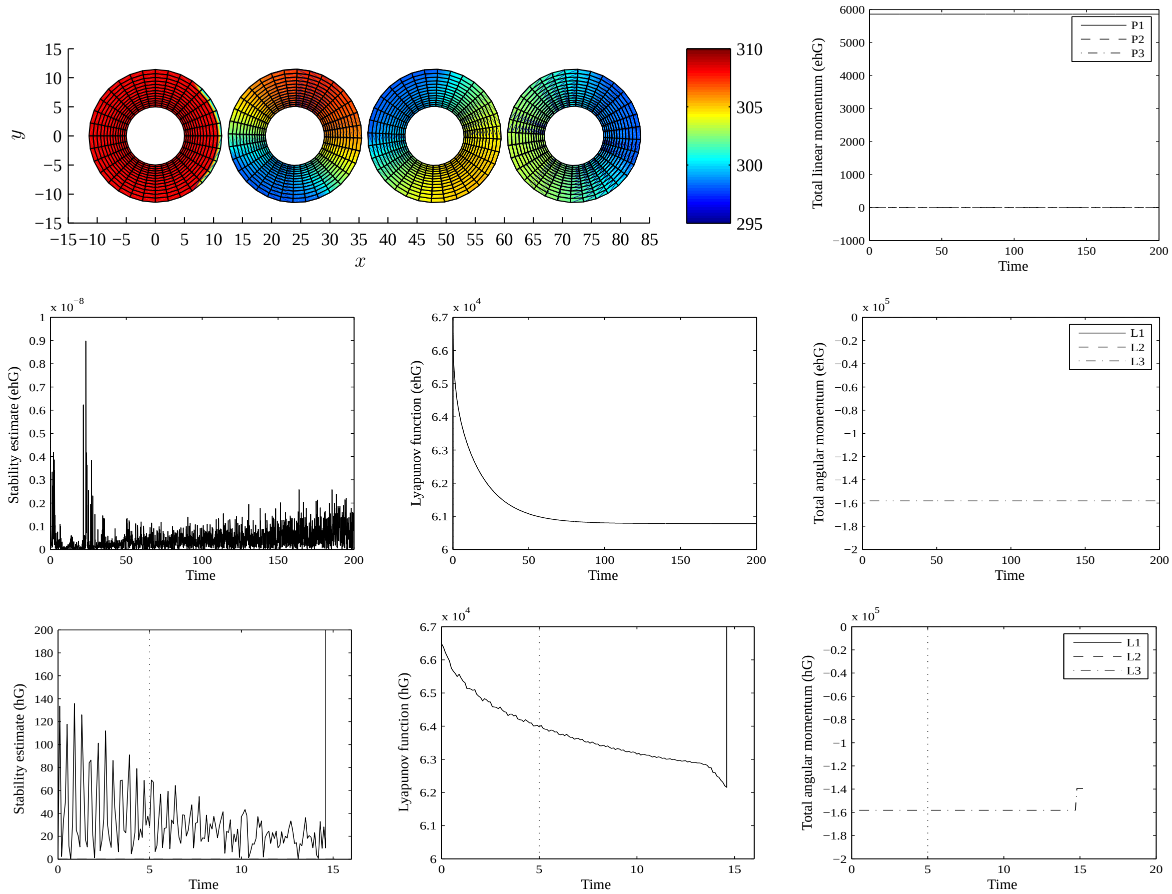

Figure 1: Free flying tyre under equilibrated external loads with a small uninsulated portion: energy-momentum-consistent ehG(1) method in the first two rows and only momentum-consistent hG(1) method in the last row.

REFERENCES

[1] Groß M., Betsch P. and Steinmann P. Conservation properties of a time FE method–Part IV: Higher order energy and momentum conserving schemes. *Int. J. Numer. Meth. Engrg.*, **63**, 1849–1897, 2005.

[2] Armero F. Energy-dissipative Momentum-conserving Time-Stepping Algorithms for Finite Strain Multiplicative Plasticity. *Comput. Meth. Appl. Mech. Engrg.*, **195**, 4862–4889, 2006.

[3] Noels L., Stainier L. and Ponthot J. P. An Energy-Momentum Conserving Algorithm Using The Variational Formulation of Visco-Plastic Updates. *Int. J. Numer. Meth. Engrg.*, **65**, 904–942, 2006.

[4] Reese S. and Govindjee S. Theoretical and Numerical Aspects in the Thermo-Viscoelastic Material Behaviour of Rubber-Like Polymers. *Mechanics of Time-Dependent Materials*, **1**, 357–396, 1998.

[5] Bottasso C. L. and Trainelli L. An Attempt at the Classification of Energy Decaying Schemes for Structural and Multibody Dynamics. *Multibody System Dynamics*, **12**(2), 173–185, 2004.